# LABEL-FREE SENSING ON SUPPORTED LIPID BILAYERS

A Dissertation

by

AARON DOUGLASS ROBISON

Submitted to the Office of Graduate Studies of
Texas A&M University
in partial fulfillment of the requirements for the degree of

DOCTOR OF PHILOSOPHY

Approved by:

| | |
|---|---|
| Chair of Committee, | Paul S. Cremer |
| Committee Members, | David H. Russell |
| | Christian Hilty |
| | George R Welch |
| Head of Department, | David H. Russell |

December 2012

Major Subject: Chemistry

# ABSTRACT

Cell membranes are integral for many biological processes. In addition to containing and protecting cellular contents and maintaining the chemical integrity of the cell, these interfaces host a variety of ligand-receptor interactions. These ligand-receptor interactions are important for cell signaling and transport and the ability to monitor them is key to understanding these processes. In addition, therapeutics and drug discovery is also aided by membrane-specific study, as the majority of drugs target receptors associated with the cell surface.

The cell membrane can be effectively mimicked by the use of supported lipid bilayers, which provide a robust platform exhibiting the lateral fluidity and composition associated with cell membranes. The ability to study both ligand-receptor interactions as well as small molecule-membrane interactions on these model membranes is aided by the fact that these assays can be multiplexed and are amenable to use with low sample volumes with high throughput.

Our laboratory has recently developed a strategy for fluorescent microscopy studies of ligand-receptor interactions on supported lipid bilayers without the use of fluorescently-labeled analytes. This technique involves the incorporation of pH-sensitive fluorophores into the composition of the supported lipid bilayer as embedded reporter dyes. It was determined that this assay can operate as either a “turn-on” or a “turn-off” sensor depending on the analyte to be detected. It was additionally found that

modulating the ionic strength of the operating buffer allows for tuning the operating pH and sensitivity of the assay.

This label-free technique can be utilized to monitor small peptide interactions with bilayers containing specific phospholipids. Basic amino acid sequences which are associated with transporting contents across membranes or anti-microbial activity can be monitored binding to negatively charged bilayers without the use of labels. Not only is this a sensitive technique for detecting small peptides, but thermodynamic data can be extracted as well.

In a final set of experiments, the interaction of proteins with phosphatidylserine (PS) in supported lipid bilayers is observed by utilizing PS-$Cu^{2+}$-induced quenching of fluorophores. Disruption of this metal-phospholipid, specifically by $Ca^{2+}$-dependent protein kinases, results in a turn-on fluorescent assay, which can be used to monitor the binding of the protein to PS and the effects of other metal interference.

.

# DEDICATION

This dissertation is dedicated to the people who have been so influential to me in the past five years. I would not have endeavored such an undertaking had it not been for my wonderful wife Andrea who was always supportive of my seemingly insane dedication to the task of research. I could not, nor would I have especially wanted to do this without her. I would also like to dedicate this to the friends that I have made in the course of this process, both within the Cremer group and within the Chemistry Department. Finally I would like to dedicate this to my daughter, whose imminent arrival has been an inspiration to finish this process

# ACKNOWLEDGEMENTS

I would like to thank my committee chair, Dr. Paul Cremer, for his guidance and encouragement. His enthusiasm and love of discovery greatly helped move me through some of the despairs inherent to this process. I would also like to thank my committee members, Dr. David H. Russell, Dr. Christian Hilty, and Dr. George R. Welch for challenging my ideas and understanding in seminars and defenses throughout the years, and helping me to become a better scientist.

I would like to thank those who went before me, especially Dr. Hyunsook Jung and Dr. Chris Monson who taught me much about this research, Dr. Wei-Ssu Liao, Dr. Keith Chang, and Dr. Jaibir Kherb who both encouraged and befriended me as a new member of the lab. Dr. Michael Eller and Dr. Michael Grubb who entered the program along with myself and were good friends throughout its course. I would like to acknowledge the Cremer Group- one that has truly been a pleasure to work with and is populated with truly talented minds. I greatly appreciate all of the discussions, both scientific and otherwise, with Matt Poyton. He is a very good friend and a very good scientist. I'm glad that he chose to work in this lab and look forward to his future work. I would also like to thank Dr. Hudson Pace for his encouragement, commiseration, and genuine friendship over the past five years. He has been a worthy Minotaur opponent, a remarkable researcher, and most importantly a very good friend. A friend one is lucky to have made. Thanks to N.W. for keeping me attuned to that aspect of my life, and to Mr. Capestrano, Joe Pasteroni and the rest from Adobe Skyscraper.

# TABLE OF CONTENTS

# LIST OF FIGURES

Page

# LIST OF TABLES

Page

# CHAPTER I

# INTRODUCTION

**Objective.** Cell membranes are integral for many biological processes. In addition to containing and protecting cellular contents and maintaining the chemical integrity of the cell, these interfaces host a variety of ligand-receptor interactions. Because the majority of drugs target cell membrane-associated receptors[1], being able to monitor ligand-receptor interactions on the cell membrane aids in therapeutic and drug discovery efforts. The ability to monitor membrane interactions is also key to understanding such phenomena as polyvalent binding[2] and association of proteins and small peptides with specific phospholipids[3,4] (Figure 1.1). Traditionally, the use of fluorescent tags has been employed to monitor ligand receptor interactions on membrane surfaces.[5-7] Indeed, our laboratory has made use of this technique to investigate the effect of hapten density[8] and presentation[9] on antibody binding. However, employing fluorescent labels can be costly and inefficient and may alter analyte behavior[10,11] especially in the case of small peptides.[12]

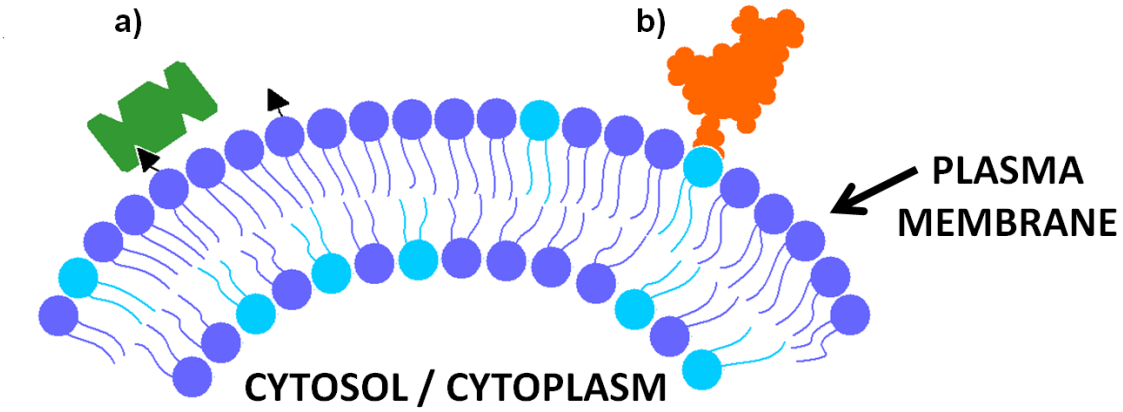


***Figure 1.1.*** Schematic of Ligand-Receptor Interaction on Cell Membrane. Illustration shows (a) protein-ligand and (b) protein-phospholipid interactions on a cell membrane.

To avoid the possible interference of labels, spectroscopic techniques have been developed for monitoring interactions on surfaces such as surface plasmon resonance (SPR),[13-16] surface enhanced Raman scattering[17] and optical resonators.[18,19] In addition, some non-spectroscopic techniques have been employed as well such as quartz-crystal microbalance (QCM),[20-23] semiconducting nanowires,[24-27] and microcantilevers.[28-31] Although these techniques avoid the use of interfering labels, they can be costly or difficult to employ, may not be easily amenable to membrane studies, or may suffer from sensitivity compared to fluorescent techniques.[32]

Recently we have developed a technique for monitoring ligand-receptor interactions on membrane surfaces that utilizes the sensitivity of fluorescence microscopy without the use of labeling the analyte of interest.[33] This technique allows for the label-free monitoring of membranes without the need for specially modified surfaces beyond annealed borosilicate glass cover slips.[34] Essentially, this assay operates on the basis of effective pH modulation at a membrane surface upon the binding of an analyte such as a protein or antibody. The associated pH change, which is due to the charged nature of the analyte, can induce a fluorescent response from pH-sensitive fluorophores which have been incorporated into the composition of the membrane. We are interested in exploring this technique in terms of increasing signal response as well as expanding the effective pH range for operating the assay. This can be achieved through the modulation of the buffering species and ionic strength as well as through modulation of the surface charge via incorporation of charged phospholipid species.

The ability to monitor the binding of small basic peptides to bilayers is of interest for many reasons. Sequences of basic residues are ubiquitous with many membrane-associated proteins,[35] especially on regions of the proteins associated with the cytoplasmic side of the membrane where there is a greater distribution of negatively charged phospholipids.[36,37] Additionally, cell-penetrating peptides (CPP's), which can aid in the delivery of species across membranes[38-41] contain basic amino acid sequences which are believed to facilitate delivery by first associating with negatively charged phospholipids in membranes. Basic residue sequences are also associated with anti-microbial peptides,[42] the understanding of which will greatly help in contending with multidrug antibiotic resistance. Techniques such as electrophoretic mobility, dye release assays, and even molecular dynamics have been utilized to study the manner in which these peptides associate and affect plasma membranes. We wish to utilized the previously described label-free technique as a simple and novel way to observe the interaction of short basic peptide sequences with bilayers in hopes of extracting kinetic and thermodynamic data. The utilization of microfluidics also helps in this regard, as low sample volumes can be used for these assays.

Phosphatidylserine (PS), a negatively charged phospholipid found in membranes that is involved in important communication events such as signaling the elimination of apoptotic cells, is also the major anionic eukaryotic phospholipid constituent.[43] In addition to being a signaler for cell apoptosis, PS also functions as a highly specific binding target for coagulation proteins such as prothrombin in the clotting cascade.[44] Other PS-specific proteins include anticoagulant annexin V[45] and conventional protein

kinase C (PKC),[46,47] both of which involve $Ca^{2+}$-dependent coordination with PS. The ubiquitous nature of PS as a signaling lipid involved in such varied processes makes it an interesting candidate for bilayer studies, especially with regards to the $Ca^{2+}$-dependent kinase. These phosphorylation enzymes contain a PS-specific binding motif referred to as the C2 domain which in addition to interacting with $Ca^{2+}$ dependently with PS binding has shown competitive binding of contaminant metals such as $Pb^{2+}$.[48]

We have recently determined that PS reversibly binds $Cu^{2+}$ with extremely high affinity.[49] This PS- $Cu^{2+}$ complex exhibits quenching of fluorescent dyes incorporated into the same bilayer, a phenomenon that we seek to exploit as a sensor for PS-binding proteins. In this strategy, the disruption of the 2:1 PS: $Cu^{2+}$ complex can lead to de-quenching of phospholipid-conjugated fluorophores and act as a turn-on sensor. Not only does this allow for the label-free study of PS-binding motifs such as the C2 domain of PKC, but it also allows for information to be gained in regards to competition with $Cu^{2+}$ for serine binding.

**Supported Lipid Bilayers.** Supported lipid bilayers (SLB's) are synthetic mimics of cell membranes and share the same phospholipid constituents thereof. Their composition can be tailored to incorporate specific ligands or phospholipid species, while maintaining the two-dimensional fluidity found in cell surfaces.[34] These bilayers can form via spontaneous vesicle fusion[50,51] and exist on a thin layer (10-20 Å) of water separating the lower leaflet and the solid support (Figure 1.2), allowing for unimpeded lateral lipid

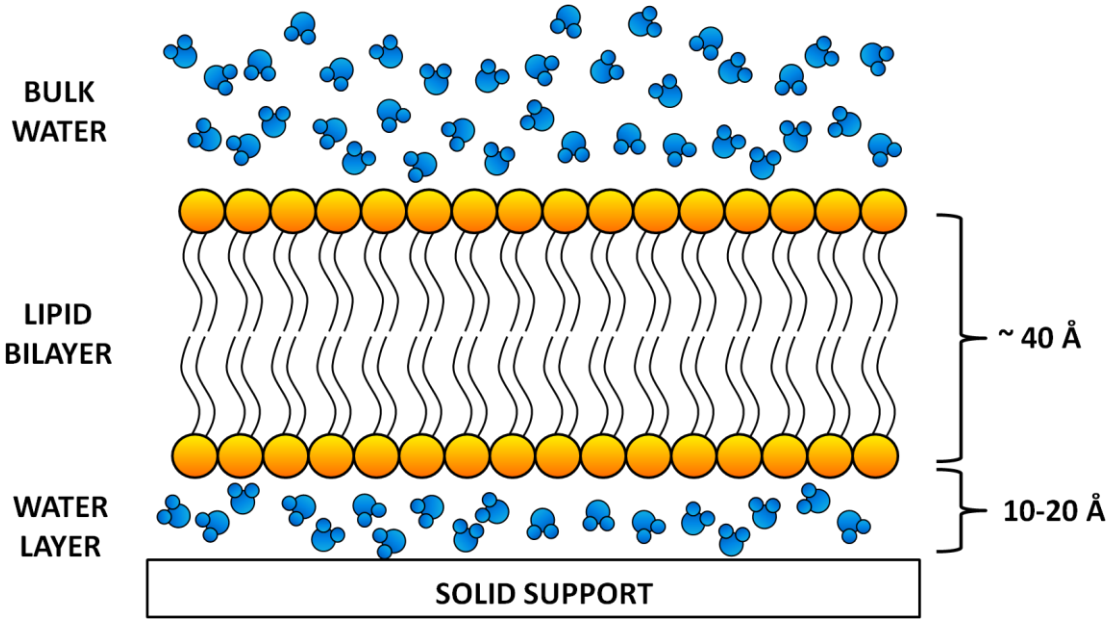


***Figure 1.2.*** Schematic of Supported Lipid Bilayer. Diagram shows a supported lipid bilayer on a hydrophilic planar substrate. The substrate usually consists of quartz or fused silica and a thin layer of water between the substrate and the lower leaflet allows for two dimensional fluidity such as that found in cell membranes.

movement.[52] Moreover, these membranes are amenable for use in multiplexed microfluidic devices.[53] Phospholipids functionalized with biotin and pH-sensitive dye have been utilized to monitor the binding of avidin and streptavidin in different buffer conditions to further understand the nature of the label-free technique described earlier. In a similar fashion, SLB's containing pH-sensitive dye and differing concentrations of phosphatidylglycerol (PG) were utilized to study the binding of short basic peptide strands and the $Cu^{2+}$-induced quenching of fluorophores in membranes was exploited with SLB's containing PS to observe the $Ca^{2+}$-dependent binding of C2 domains.

**Microfluidics and Flow Cells.** Microfluidic devices offer the ability to observe binding events on SLB's while utilizing very small sample volumes[53] and can be produced in a facile method using polydimethylsiloxane (PDMS) and glass.[54] These devices also have the inherent advantage of multiplexing many bilayer studies simultaneously to both reduce the time constraint for performing assays under multiple conditions and reduce the temporal noise associated with illumination sources.

Traditionally our laboratory has made use of total internal reflection fluorescence microscopy (TIRFM) in conjunction with bilayer studies in microfluidics.[8,9,55] However, since the studies performed herein are performed in a label-free manner, TIRFM can be replaced with traditional epifluorescence microscopy techniques, as illustrated in Figure 1.3. After a PDMS mold is fabricated via soft lithographic techniques[56] it is attached to an annealed glass cover slip after being rendered hydrophilic by treatment with oxygen plasma. Bilayers are formed inside the microfluidic channels via the vesicle fusion

technique[53] after which the desired buffer or protein solution is continually flowed though by gravity-driven flow. These bilayers can be monitored in real time with an inverted fluorescence microscope, allowing for facile determination of equilibration in binding experiments. This is advantageous, especially in regards to low concentrations where, as opposed to bulk solutions limited by diffusion, flow through microfluidics is laminar, resulting in a small no-slip region near the surface through which diffusion of analyte occurs rapidly.[57]

Another method for analyzing bilayers in real time under flowed conditions is the use of simple flow cells, made of circular PDMS wells ~ 1.5 μm deep which contain μL of total volume. These wells can be patterned with fibrinogen and simple PDMS micro-contact techniques.[58] Although these flow cells lack the minute volume and ease of multiplexing that microfluidics offer, they are useful for avoiding complications with small PDMS channels.[59]

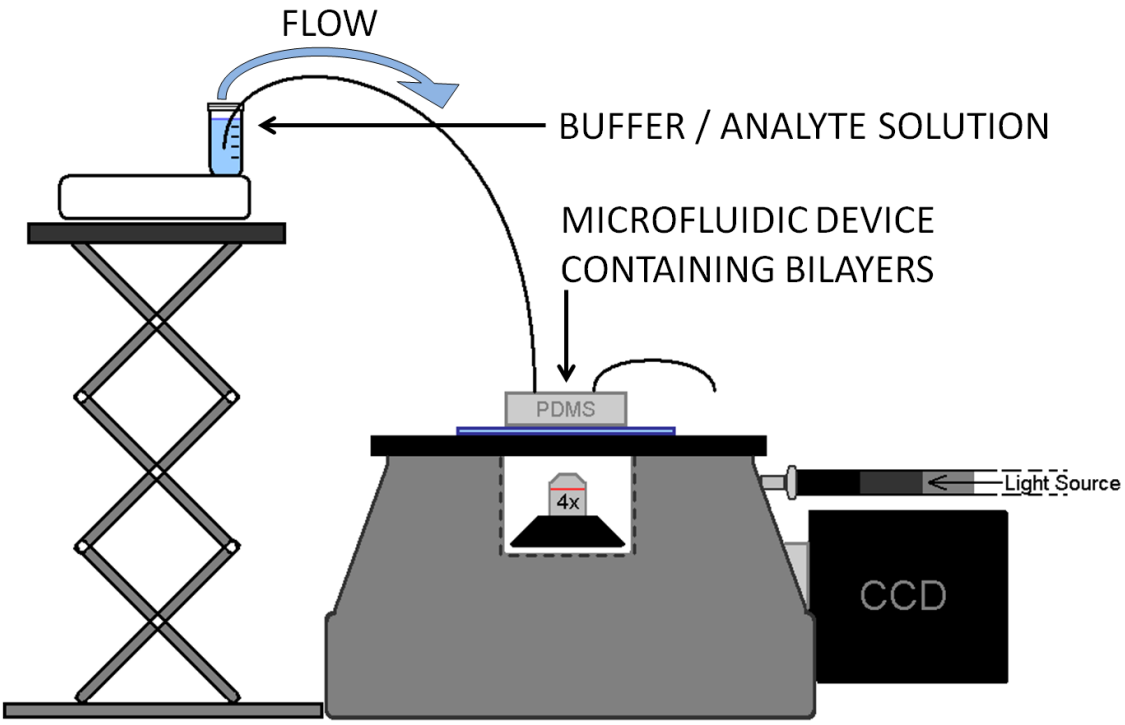


***Figure 1.3.*** Schematic of Fluorescence Microscopy Setup. Illustration shows a typical microfluidic epifluorescence microscopy experimental setup. Solution is delivered to each microfluidic channel via gravity driven flow through polytetrafluoroethylene tubes. The microfluidic channels are monitored in real time with an inverted fluorescent microscope.

# CHAPTER II

# EXPERIMENTAL SECTION

**Materials.** 1-palmitoyl-2-oleoyl-sn-glycero-3-phosphocholine (POPC), 1-palmitoyl-2-oleoyl-sn-glycero-3-phospho-(1'-rac-glycerol) (sodium salt) (POPG), 1,2-dioleoyl-sn-glycero-3-phospho-L-serine (sodium salt) (DOPS), 1-hexadecanoyl-2-(9Z-octadecenoyl)-sn-glycero-3-phosphoethanolamine) (POPE), and (1,2-dipalmitoyl-sn-glycero-3-phosphoethanolamine-N-(cap biotinyl) (sodium salt) (biotin-cap PE) were all purchased from Avanti Polar Lipids (Alabaster, AL). Lissamine rhodamine B sulfonyl chloride and Oregon Green® 488 1,2-dihexadecanoyl-sn-glycero-3-phosphoethanolamine (Oregon Green® 488 DHPE) were both purchased from Invitrogen (Eugene, OR).

Streptavidin and avidin were both purchased from Rockland (Gilbertsville, PA) and bovine fibrinogen was purchased from MP Biomedicals (Solon, OH). Phosphate buffers, sodium chloride, and MES buffer was purchased from Sigma-Aldrich (St. Louis, MO). Calcium chloride and copper(II) chloride were purchased from Acros (Pittsburgh, PA). Amidated nona-lysine (K9) was purchased from GenScript (Piscataway, NJ). Amidated nona-lysine and nona-arginine (R9) were provided by the Pellois Laboratory at Texas A&M University, and protein kinase C2-α was provided by the Igumenova Laboratory at Texas A&M University.

Purified water was obtained from a NANOpure Ultrapure Water System (18.2 MΩ·cm, Barnstead). Glass cover slips used as supports for bilayers were purchased from

Fischer Scientific (24 x 40 mm, No. 1.5) and polydimethylsiloxane (PDMS, Dow Corning Sylgard Silicone Elastomer-184), used for microfluidics and flow cells, was obtained from Krayden, Inc (El Paso, TX). Hydrofluoric acid and thin layer chromatography (TLC) plates (silica gel 60 F254) were purchased from EMD (Philadelphia, PA) and ammonium fluoride was purchased from Alfa Aesar (Ward Hill, MA). Polytetrafluoroethylene (PTFE) tubing (inner diameter 0.66 mm) was purchased from SPC Technology (Chicago, IL).

**Synthesis and Separation of Dye-Conjugated Phospholipids.** To synthesize rhodamine B-POPE phospholipids, a primary amine reaction was utilized by mixing a solution of 10 mg of rhodamine B sulfonyl chloride in 1 mL of chloroform with 10 mg of POPE and 2 μL of diethylamine. The reaction was stirred for one hour at room temperature. After the reaction, the solution was spotted onto a TLC plate (EMD, 5715-7, silica gel 60 F254) and developed with a chloroform:methanol mixture (92:8) to obtain rhodamide-B labeled POPE. The mixed isomers of rhodamine B-POPE could be further separated on another TLC plate developed with ammonium hydroxide solution: n-propanol (35: 65). The reaction was confirmed with matrix-assisted laser desorption ionization mass spectrometry (Figure 2.1).

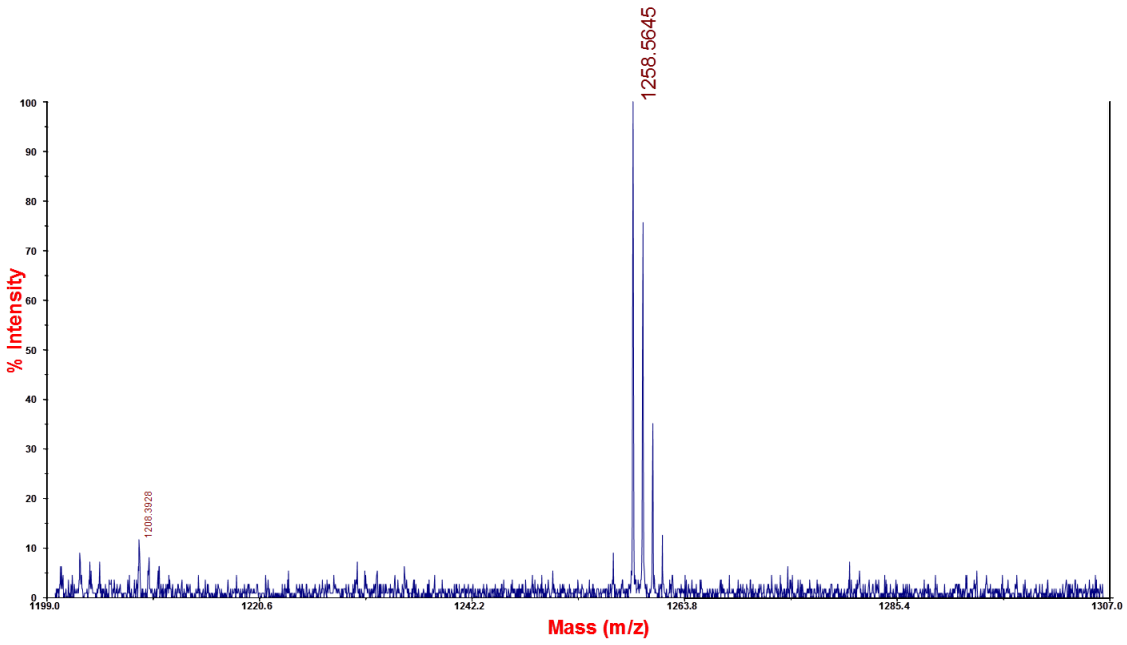


***Figure 2.1***. Mass Spec Confirmation of Dye-Conjugated Phospholipid. Matrix assisted laser desorption ionization mass spectrum showing a peak at 1258.6 (rhodamine-B POPE + 2H+).

**Preparation of Small Unilamellar Vesicles.** To make small unilamellar vesicles, first a mixture of the desired phospholipids were mixed in chloroform before being dried by purging with nitrogen gas. The mixtures were then desiccated under vacuum for three hours before being reconstituted in 10 mM phosphate buffer with 150 mM NaCl to a concentration of 0.5 mg/mL. After the lipids were fully dissolved in the buffer solution, they were subjugated to ten freeze-thaw cycles by immersion in liquid nitrogen and warm water. This was followed by at least seven extrusions using a Lipex extruder (Northern Lipids Inc., Vancouver, Canada) through two stacked polycarbonate filters (Whatman) with 100 nm hole diameters. Size of the extruded vesicles was determined by dynamic light scattering (Brookhaven Instruments 90Plus Particle Size Analyzer) with typical sizes between 90 and 100 nm. Vesicle solutions were stored at 4 ºC until use. Structures of the phospholipids utilized in these studies are shown in Figure 2.2.

**Preparation of Glass Substrates.** Glass substrates for accommodating lipid bilayers were prepared from Fischer glass cover slips (24 x 40 mm, No. 1.5) by first boiling in a 1:6 solution of 7X cleaning solution (MP) and water for at least one hour. This was followed by rinsing with copious amounts of purified water before drying thoroughly with nitrogen gas. The cover slips were then annealed for five hours at 520 ºC before being stored until use.

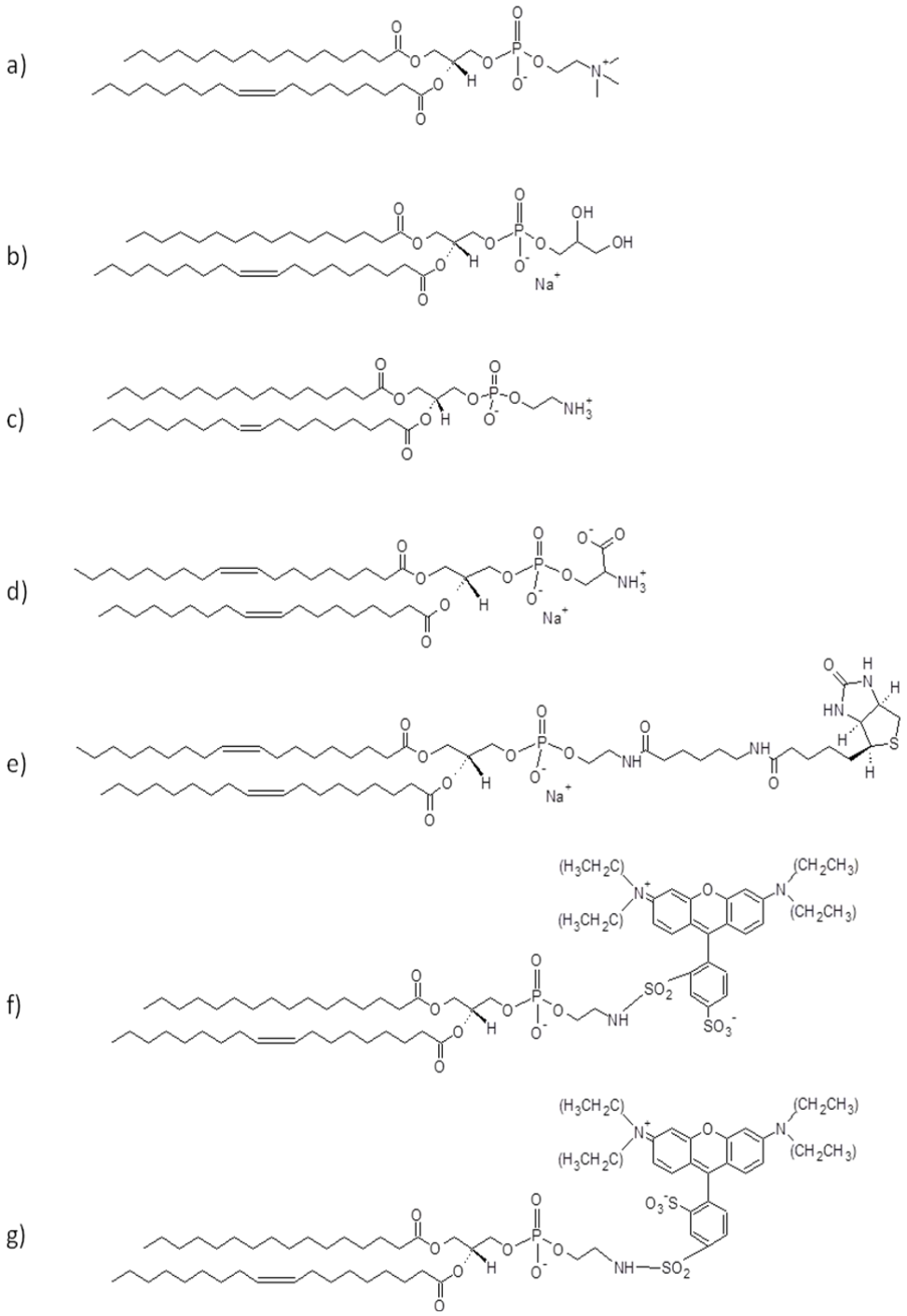


***Figure 2.2.*** Structures of Relevant Phospholipids**.** Structures of a) POPC, b) POPG, c) POPE, d) DOPS, e) DOPE-biotin cap, f) *ortho*-rhodamine B, and g) *para*-rhodamine B.

**Fabrication of Microfluidic Devices.** Seven channel microfluidic devices with channel widths of ~120 μm and heights of ~50 μm were produced via soft lithographic techniques.[53] Glass slides (soda lime, Corning) were first cleaned by immersion for one hour in a 25:75 (v/v) mixture of concentrated hydrogen peroxide and concentrated sulfuric acid. The slides were then rinsed with copious amounts of water and dried under a stream of nitrogen. A layer of photoresist (Shipley 1827) was then spin-coated on the surface of the slides which were then exposed to UV for 12 seconds at > 400 W through an appropriate negative mask. The slides were treated with developing solution and any stray photoresist was removed with acetone before baking at 120 ºC overnight. Buffered oxide etchant (BOE) was used to etch the patterns into the glass slides. The glass was immersed in a BOE solution prepared from a 1:6 ratio (v/v) of 48% hydrofluoric acid (EMD Chemicals Inc., Germany) and aqueous ammonium fluoride (200 g in 300 mL purified water, Alfa Aesar, Ward Hill, MA) then immersed in 1 M HCl followed by rinsing with water. This process was repeated up to six times before the remaining photoresist was removed with acetone. The surface was rendered hydrophobic by vapor deposition of tricholododecylsilane. A 10:1 (v/v) mixture of Sylgard silicone elastomer-184 and a curing agent were degassed under vacuum before being poured over the glass pattern. This polymer was then cured for one hour at 70 ºC before being peeled off of the glass surface. The polymer and a glass cover slip which had been prepared as described previously were then treated with 25 W oxygen plasma for 30 seconds before being brought into contact, forming the PDMS microfluidic device.

**Fabrication of Flow Cells.** A sheet of PDMS 1.5 µm thick was produced by curing the polymer between two hydrophobized glass slides separated by cover slips 1.5 µm in thickness. A hole was cut into the center of the PDMS sheet and the well was placed on a clean coverslip. A PDMS stamp which was cured over a seven channel microfluidic pattern was incubated in a 1 mg/mL bovine fibrinogen solution, then pressed onto the glass cover slip in the well and allowed to set for five minutes before being removed. Vesicles were then deposited in the well and incubated for ten minutes before being rinsed with copious amounts of water. A second sheet of PDMS with an inlet and an outlet hole was then placed on top of the well, and the entire structure was held together by aluminum plates with two clips. Solution was flowed through the device as experiments were performed.

**Formation of Supported Lipid Bilayers.** Vesicle solutions were diluted 1:1 with 1 M NaCl before being introduced to microfluidic channels. These were allowed to incubate for at least ten minutes before being rinsed with buffer to remove excess vesicles. The fluorescence of each bilayer was able to be monitored as buffer was flowed over it to ensure that equilibration had been achieved before any experimental additions were made. Precautions were taken to avoid the introduction of any air bubbles into the channels. Likewise, flow rates were kept so that bilayers were not damaged, usually achieving rates of ~50 µL/hr.

**Measurement of pH Titration Curves.** Titration curves for various bilayer and buffer conditions were performed within microfluidic devices or flow cells. After bilayers had been deposited, buffer of specific pH which had been previously prepared and measured with a pH meter (Orion 3-Star, Thermo Scientific) was flowed into the microfluidic or flow cell. The phosphate buffers with (or without) NaCl were produced by combining appropriate amounts of $NaH_2PO_4$, $Na_2HPO_4$, and $Na_3PO_4$. Fluorescence was allowed to stabilize before a new pH buffer was flowed and fluorescent micrographs were captured with a Nikon Eclipse Ti-U fluorescence microscope (Tokyo, Japan) equipped with a ProEM 1024 CCD camera (Princeton Instruments) and a 4x air objective (N.A.=0.13). The fluorescence measurements were normalized to the maximum value and the data set was fit with a four parameter logistic curve:

$$y = y_{min} - \frac{y_{max} - y_{min}}{1 + 10^{(logK - x)H}}$$

where y is the fluorescence intensity, x is the pH, K is the inflection point which corresponds to the apparent pKa and H is the Hill slope.

**Fluorescence Microscopy Measurements.** Fluorescence measurements were made with an inverted Nikon Eclipse Ti-U fluorescence microscope (Tokyo, Japan) equipped with a ProEM 1024 CCD camera (Princeton Instruments) and a 10x air (N.A.= 0.45) objective. A Texas Red filter set (Chroma Technology, Bellows Falls, VT) was used with a Lumen 200 (Prior Scientific) light source. All fluorescent images were processed with MetaMorph software (Version 7.7.0.0, Universal Imaging).

# CHAPTER III

# TURN-ON AND TURN-OFF SENSING OF PROTEIN-LIGAND BINDING BY MODULATING BUFFER CONDITIONS

**Introduction.** The ability to monitor ligand-receptor interactions is a necessity for biotechnological advances as well as a fundamental understanding of cell biology. The single-molecule sensitivity that fluorescent labeling can provide and the relative ease of fluorescence measurements has resulted in the utilization of this technique for detecting and monitoring proteins and nucleotides. Fluorescent labels can, however, interfere with analyte activity and can be difficult to efficiently employ.[10,11] Many sensing techniques have consequently been developed such as quartz-crystal microbalance (QCM),[20-23] surface plasmon resonance (SPR),[13-16] semiconductor nanowire conductivity,[24,25] and optical microcavities that avoid the use of fluorescent labels.[18] Although these techniques avoid the problems associated with directly attaching fluorescent tags to analytes, they can behave non-linearly in response to analyte concentration, require specialized equipment or procedures which can be difficult and/or costly to employ, or possess poorer detection limits than fluorescence techniques.

It is advantageous to be able to monitor ligand-receptor interactions on supported lipid bilayers[60] because these platforms effectively act as a simplified cellular surface, incorporating the same lipid molecules as well as maintaining two-dimensional lipid fluidity.[34] Indeed, the majority of current drug target ligands are associated with the cell surface,[1] making the ability to effectively monitor such systems key for therapeutics and

drug discovery. Consequently, much work has been done to produce supported lipid bilayers that mimic the cellular surface with various supports[61-64] or tethers.[65-70] With the incorporation of microfluidic devices,[53] such supported lipid bilayer systems can be produced in a rapid and facile method while utilizing only small amounts of analyte. Heterogeneous flow-based microfluidic techniques also afford the ability to change parameters such as ionic strength or buffer pH and monitor fluorescent response in real time. The ability to utilize glass substrates as membrane supports is also advantageous as these surfaces can readily accommodate fluid lipid bilayers[50,51] via simple and rapid vesicle fusion.

Recently, we have developed a sensing technique that utilizes the sensitivity of fluorescent measurements while avoiding the complications of directly labeling the analyte of interest.[33] This technique involves the incorporation of a pH sensitive dye, *ortho*-conjugated Texas Red DHPE (Texas Red 1,2-dihexadecanoyl-*sn*-glycero-3-phosphoethanolamine, triethylammonium salt), into a supported lipid bilayer containing the ligand biotin-PE (1,2-dipalmitoyl-sn-glycero-3-phosphoethanolamine-N-(cap biotinyl) (sodium salt)). This isomer of Texas Red loses fluorescence when it is deprotonated at higher pH, while the *para*-conjugated isomer retains its fluorescence and therefore serves as a reference dye.[71] Upon the binding of a negatively charged protein, the effective pH near the binding event will be lowered due to the protein's recruitment of hydronium ions, thus causing protonation and increased fluorescence in the *ortho*-Texas Red isomer. This "turn on" sensing approach was demonstrated using the biotin/anti-biotin binding pair.[33]

Herein, we have utilized the *ortho* isomer of rhodamine B (Lissamine rhodamine B sulfonyl chloride, mixed isomers) conjugated to the free amine of POPE (1-hexadecanoyl-2-(9Z-octadecenoyl)-*sn*-glycero-3-phosphoethanolamine) as the reporter dye incorporated into the bilayer. Rhodamine B is far less expensive and the *ortho* isomer exhibits a more complete quenching behavior at high pH compared to *ortho*-Texas Red. Additionally, the *ortho* isomer of rhodamine B exhibits pH-sensitive fluorescence at more acidic pH values compared to *ortho*-Texas Red.[72] This allows for the detection of positively charged proteins near neutral pH. The sensor works in a manner similar to the detection of negatively charged species, except that a decrease in fluorescence accompanies a binding event because the surface becomes more positively charged and the effective local pH is therefore increased (Figure 3.1). The use of avidin/biotin and streptavidin/biotin binding pairs were implemented to test these ideas in both "turn off" and "turn on" mode (Figure 3.1). Avidin has an isoelectric point (pI) of ~10.[73] It is therefore positively charged at a working pH of 7.2 and, in fact, caused a decrease in fluorescence upon membrane binding. For streptavidin, there was an increase in fluorescence upon binding as expected at pH ranges near or above the protein's reported isoelectric point 6.4,[73] while a decrease in fluorescence accompanied binding at pH values below the pI. Moreover, by modulating the ionic strength of the buffer used in this assay, it was possible to both increase the sensitivity of the detection response as

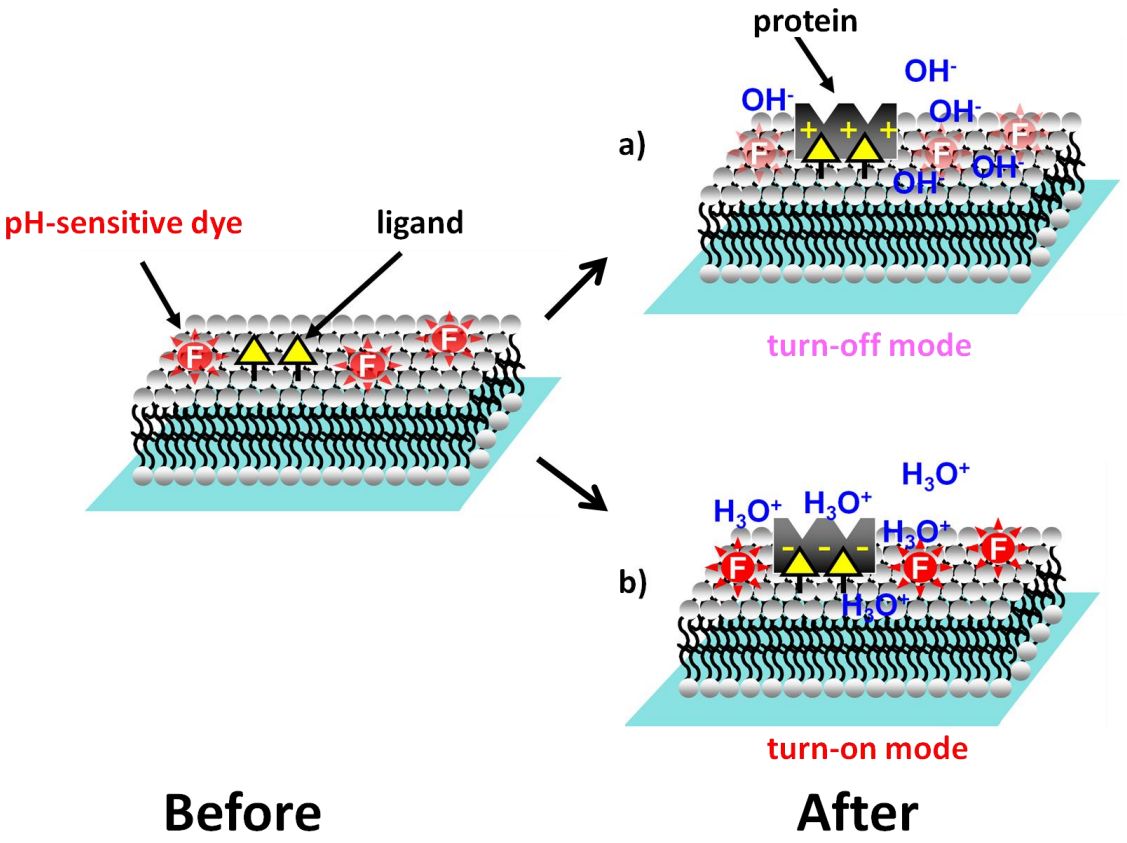


***Figure 3.1.*** Schematic of pH Modulation Assay. Illustration shows the pH modulation assay in both "turn-off" and "turn-on" mode. (a) A positively charged protein (e.g., avidin) recruits hydroxide ions upon binding and renders the membrane surface more basic, decreasing the fluorescence of the dye. (b) A negatively charged protein (e.g., streptavidin) recruits hydronium ions, and upon binding enhances the fluorescence of the dye molecules nearby by rendering the surface more acidic

well as shift the apparent pKa of the *ortho*-rhodamine B dye, offering different pH ranges for detection assays.

**pH titration curves.** Initial experiments were performed to obtain titration curves for 0.5 mol% *ortho*-rhodamine B-POPE in POPC bilayers with 0 and 5 mol% biotin PE. The pH of the bulk solution above the bilayers was altered via the continuous flow of a specific PBS solution with 150 mM NaCl and fluorescent images were captured until stabilization occurred. Once the fluorescent intensity stabilized for a given pH, the fluorescent intensity value was recorded and a different pH was flowed over the bilayer as the process was repeated (Figure 3.2). Representative intensity line scans for these measurements can be found in Figure 3.2 a. The bilayer fluorescence data was normalized to the pH value with the maximum fluorescence intensity. The intensity measurements versus pH value curves for the two bilayer conditions were fit to a sigmoidal curve (solid lines in Figure 3.2 b) and the apparent pKa values were extracted. Values of 6.2 ± 0.1, and 6.5 ± 0.1 were obtained for bilayers with 0 mol% and 5 mol% biotin-PE, respectively.

**Sensing Avidin and Streptavidin.** Next, experiments were performed with POPC bilayers containing 5 mol% biotin PE and 0.5 mol% *ortho*-rhodamine B POPE in both “turn on” and “turn off” mode. For these experiments, avidin and streptavidin were utilized as the binding analytes of interest as they both share a strong affinity for biotin.[74] Specifically, experiments were performed at pH 7.2, which falls within the linear

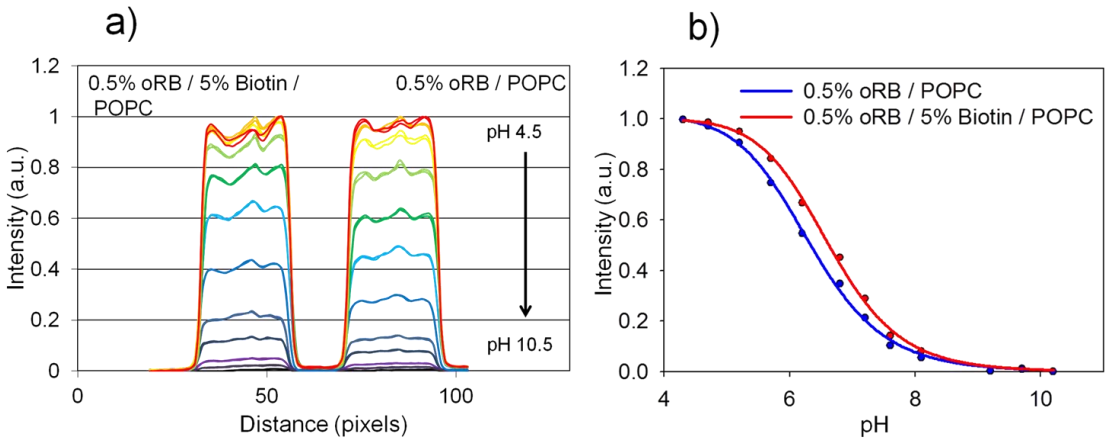


***Figure 3.2.*** Line Scans and pH Titration Curve for High Salt Buffer. pH titration: (a) Fluorescence intensity line scans across channels containing bilayers composed of 0.5 mol% *ortho*-rhodamine B POPE (oRB) and POPC with and without 5 mol% biotin. (b) Titration curves for each membrane composition. Y axis values were obtained from the intensity of the fluorescence line scan at each pH divided by the maximum fluorescence intensity for the titration. The solid circles represent individual fluorescence measurements and the solid lines are sigmoidal fits to the data.

response range of the dye as a function of pH (Figure 3.2). Under these conditions, streptavidin carries a net negative charge while avidin carries a net positive charge.[73] To perform an experiment, three parallel microfluidic channels were coated with POPC bilayers containing *ortho*-rhodamine B-POPE and biotin PE, a third control channel was coated with POPC bilayers containing *ortho*-rhodamine B-POPE, but no biotin PE (Figure 3.3 a). Fluorescent micrographs were captured every five minutes as 10 mM PBS buffer at pH 7.2 with 150 mM NaCl was flowed through each channel until stabilization occurred. 300 nM of streptavidin was then flowed into left channel, while 300 nM of avidin was flowed into the middle channel and the right channel. Data were collected every five minutes. The fluorescence intensity from each channel as a function of time is shown in Figure 3.3 b. Moreover, the individual fluorescence line scans at 0 and 65 minutes are shown in Figures 3.3 c-e. Following a 30 minute stabilization period, 300 nM protein in the same buffer was introduced to each channel. With the introduction of streptavidin, the fluorescence was increased by about 5% whereas the addition of avidin resulted in a decrease in fluorescence intensity of about 20%. The control channel showed no change in signal upon the addition of avidin. The difference in signal elicited from each protein reflects the isoelectric point of the protein and the operating pH of the experiment. Indeed, the experiment is conducted just above the isoelectric point for streptavidin, but lies far below the isoelectric point of avidin. Consequently, avidin is expected to be a more highly charged species at this pH[75] and therefore perturb the apparent local pH above the supported lipid bilayer to a much greater extent upon binding.

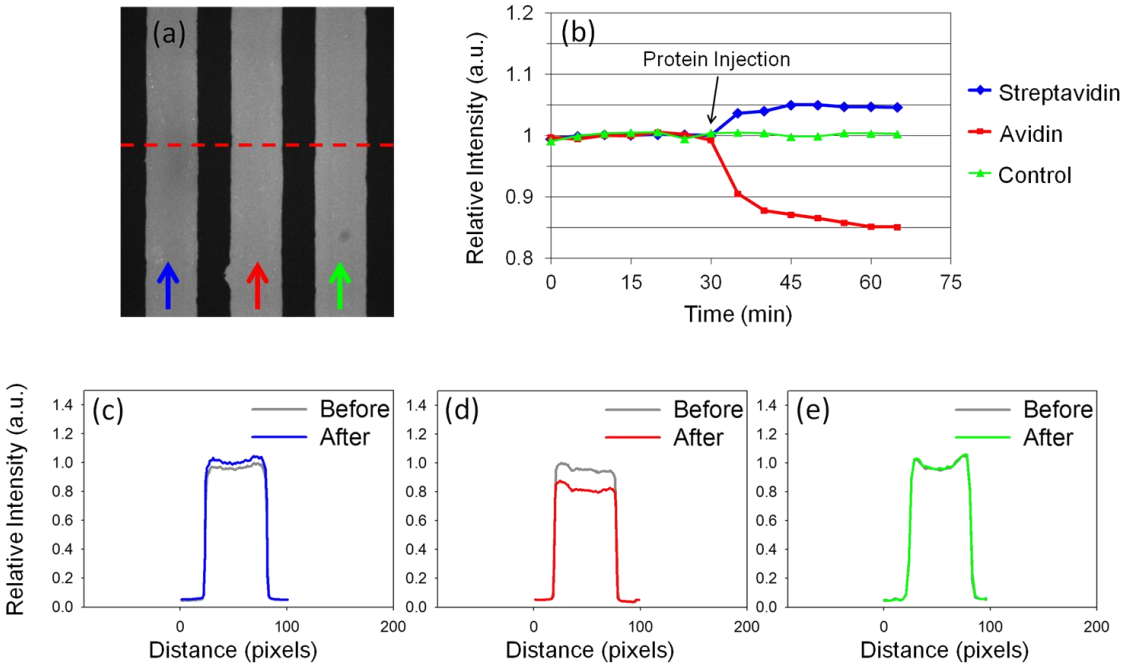


***Figure 3.3.*** Sensing of Streptavidin and Avidin Under High Ionic Strength. Protein sensing: (a) Fluorescence image of a bilayer-coated microfluidic channel containing 0.5 mol% *ortho*-rhodamine B, 5 mol% biotin PE and POPC and a control bilayer lacking biotin PE. The red dashed line corresponds to the region in which fluorescent intensity measurements were made before and after introduction of protein. (b) Average channel intensity as a function of time before and after the introduction of streptavidin (blue), avidin (red) or avidin without biotin in the bilayer (green). Experimental line profiles of the microfluidic channels before and after the addition of (c) 300 nM streptavidin, (d) 300 nM avidin and (e) 300 nM avidin to a control bilayer. A 10× air objective was used to make all measurements and experiments were run in 10 mM PBS buffer with 150 mM NaCl at a bulk pH of 7.2.

To ensure that the "turn-off" sensor for avidin was indeed due to the binding of the protein and consequential increase the local hydronium ion concentration rather than photobleaching of the dye, control experiments were carried out on biotinylated membranes utilizing the pH-insensitive *para* isomer of rhodamine B-labeled POPE with 5 mol% biotin-PE. As expected, the fluorescence intensity did not change in this assay (Figure 3.4).

**Altering Buffer Conditions to Optimize Assay.** To probe the effect of salt screening on fluorescence response, experiments were carried out using 10 mM PBS without NaCl. This resulted in a buffer with decreased ionic strength and consequentially an increased Debye length.[76] This should enhance the sensitivity of the assay by effectively increasing the area of the bilayer that will be influenced by the binding of a protein. Specifically, under high salt conditions (150 mM NaCl) in a 10 mM PBS buffer, the Debye length is about 6.6 Å.[76] When a 10 mM PBS buffer is used without NaCl, the Debye length increases to about 12.4 Å, providing each protein a greater range of influence on reporter dyes in the proximity. A titration curve performed under these conditions on bilayers consisting of 0.5 mol% *ortho*-rhodamine B, 5 mol% biotin-PE in a POPC matrix resulted in a shift in the apparent pKa of *ortho*-rhodamine B dye by about 1 pH unit, as can be seen in Figure 3.5. The line scans from which these titration curves were created can be seen in Figure 3.6. This shift is not surprising, considering that decreasing the ionic strength of a solution should lead to an increase in the apparent pKa of a titratable species as predicted by Debye-Hückel theory.[77] This condition

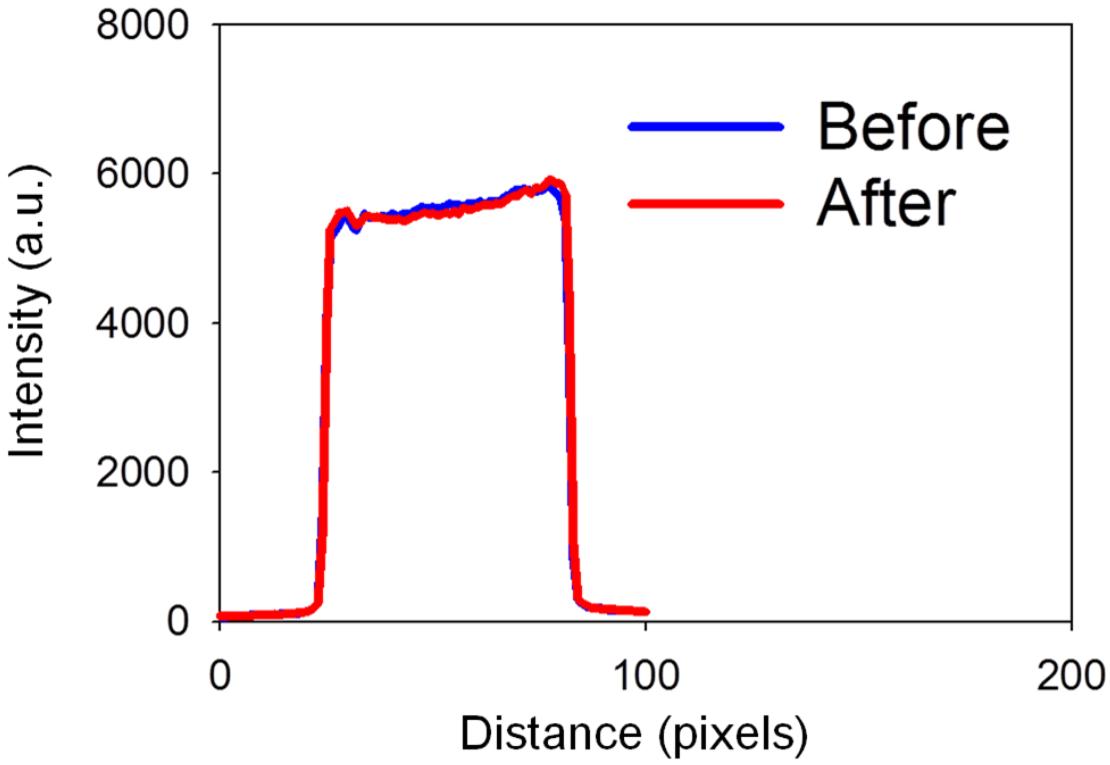


***Figure 3.4.*** Scan for *para*-Rhodamine B Control Assay**.** Fluorescence intensity line profile data corresponding to a bilayer composed of 5 mol% biotin and 0.5 mol% *para*-rhodamine B-POPE in POPC before and after the addition of 300 nM avidin. 10 mM PBS with 150 mM NaCl at pH 7.2 was used

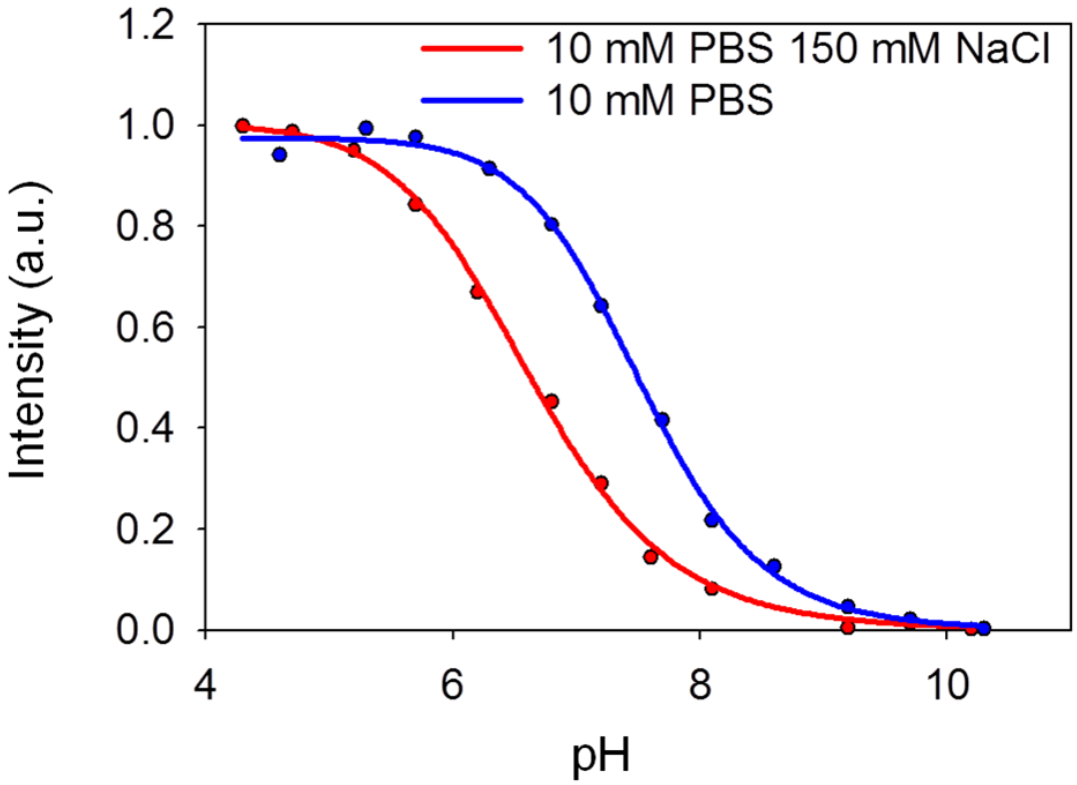


***Figure 3.5.*** pH Titration Curves for High and Low Ionic Strength Buffers**.** Titration curves for two buffer conditions with supported POPC bilayers containing 0.5 mol% *ortho*-rhodamine B and 5 mol% biotin-PE. The Y-axis values were obtained from the intensity of the fluorescence at each pH divided by the maximum fluorescence intensity for the titration. The solid circles represent individual fluorescence measurements, and the solid line is a sigmoidal fit to the data.

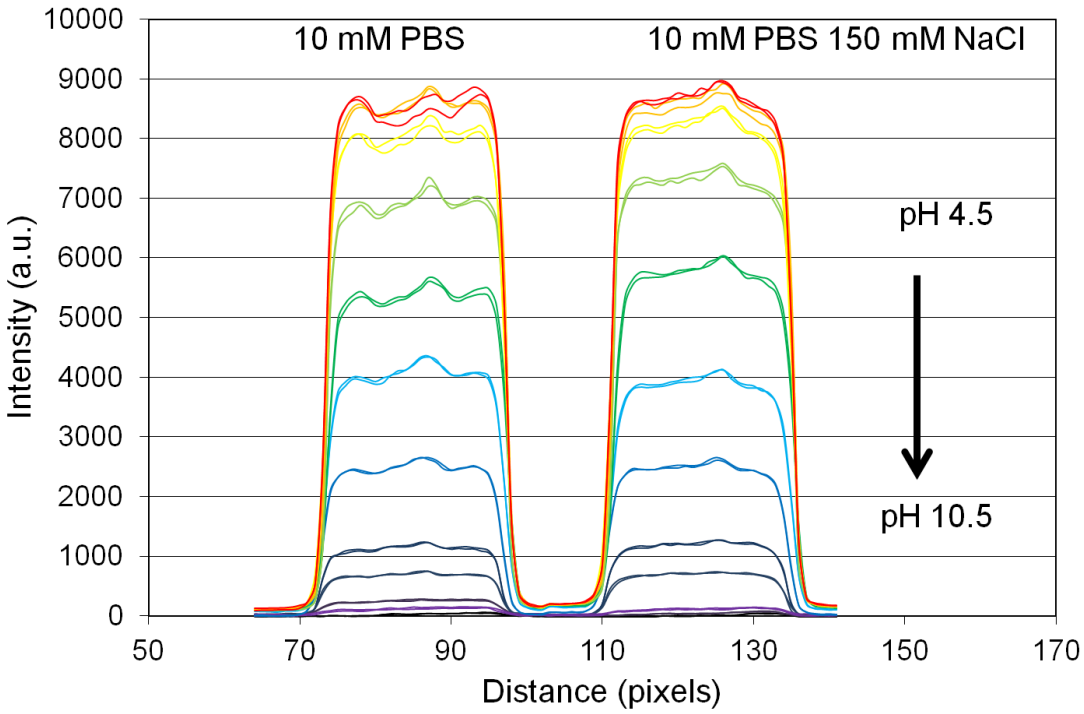


***Figure 3.6.*** Line Scans for pH Titration Curves in Figure 3.5. Fluorescence intensity line profile data from which titration curves were extracted in Figure 3.5.

consequentially shifts the linearly-responsive pH range so that experiments can be run at a pH of 8.1, where streptavidin is more negatively charged, but avidin is somewhat less positively charged.

To test low ionic strength conditions on sensor response, bilayers were formed inside two parallel microfluidic channels with and without 5 mol% biotin-PE. The bilayers were rinsed with 10 mM PBS until the fluorescence stabilized. Next, 300 nM streptavidin was introduced to the bilayers in a pH 8.1 buffer composed of 10 mM PBS and 150 mM NaCl and flowed for 30 minutes until the fluorescence response stabilized. Following the incubation, the channels were flushed with 10 mM PBS buffer until the signal stabilized again. Identical experiments were also performed with avidin. As can be seen in Figure 3.7, the introduction of streptavidin resulted in an increase in fluorescence whereas the introduction of avidin resulted in a fluorescence decrease. Because this assay was run at a lower ionic strength, there is concern that non-specific adsorption may occur due to electrostatic interaction between the protein and the bilayer, leading to signal from biofouling. However, the control channel in each channel pair, which lacked biotin, demonstrated that any non-specific adsorption was very low under these conditions.

The relative change in signal under each set of conditions is provided in Table 3.1. As can be seen, this was a factor of three for streptavidin from high ionic strength conditions to low ionic strength conditions. The change was even larger for avidin, a factor of six. This is quite curious as streptavidin should contain a higher negative charge at pH 8.1 compared with 7.2 as it is further from its isoelectric point. Therefore, signal

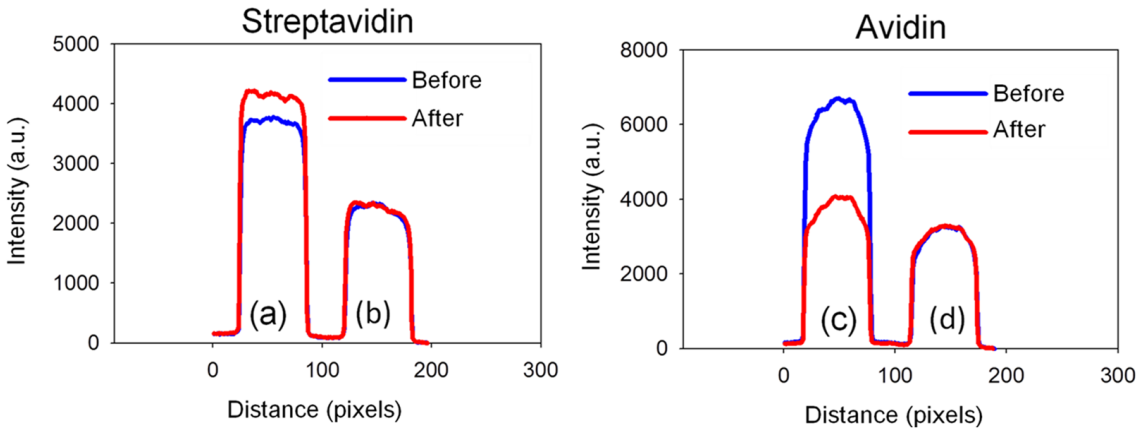


***Figure 3.7.*** Sensing of Streptavidin and Avidin Under Low Ionic Strength**.** Protein sensing in 10 mM PBS: Line scans for microfluidic channels before and after the addition of streptavidin or avidin. (a) Bilayer composed of 0.5 mol% *ortho*-rhodamine B and 5 mol% biotin-PE in POPC before and after the addition of streptavidin. (b) Control bilayer composed of 0.5 mol% *ortho*-rhodamine B in POPC before and after addition of streptavidin. (c) Bilayer composed of 0.5 mol% *ortho*-rhodamine B and 5 mol% biotin-PE in POPC before and after the addition of avidin, and (d) control bilayer composed of 0.5 mol% *ortho*-rhodamine B in POPC before and after addition of avidin.

**Table 3.1.** Summary of Protein Signal at Different Sensing Conditions.

| Protein | Experimental Conditions | Average Ending Signal with Respect to a Starting Signal of 1.0 |
|---|---|---|
| Streptavidin | 10 mM PBS 150 mM NaCl, pH 7.2 | +1.07 |
| | 10 mM PBS, pH 8.1 | +1.21 |
| | 10 mM PBS 150 mM NaCl, pH 5.9 | -0.95 |
| Avidin | 10 mM PBS 150 mM NaCl, pH 7.2 | -0.88 |
| | 10 mM PBS, pH 8.1 | -0.26 |

should increase on both protein charge as well as ionic strength grounds. By contrast, avidin should be closer to its isoelectric point at pH 8.1 than at 7.2. Therefore, a higher response is only expected because of the reduced screening, while the lower protein charge should actually lead to reduced signal.

To separate the effects of ionic strength and pH, a final set of experiments was designed, in which the fluorescence response was monitored as a function of pH at constant ionic strength for streptavidin. Because the isoelectric point for this protein is near neutral pH, it is expected that the assay should change from turn-on to turn-off

mode if the assay is run at sufficiently acidic pH. To test this idea, supported POPC bilayers were form with 0.5 mol% ortho-rhodamine B and 5 mol% biotin-PE in two parallel microfluidic channels. In each case, the solution contained 10 mM PBS with 150 mM NaCl, but the experiments were run at pH 5.9 and 7.4. Data in Figure 3.8 displays the results. For the first 30 minutes, pure buffer at each respective pH was flowed over the system in the absence of protein. This provided a fluorescence intensity benchmark with which to compare protein-bound conditions. Following stabilization, 300 nM streptavidin diluted into the respective rinsing buffer was flown into each channel. As can be seen, pH 7.3 showed an intensity increase compared with the absence of protein, but pH 5.9 showed a decrease, which is consistent with the macromolecule being below its isoelectric point. Thus, turn off behavior is observed under these more acidic conditions (Table 3.1).

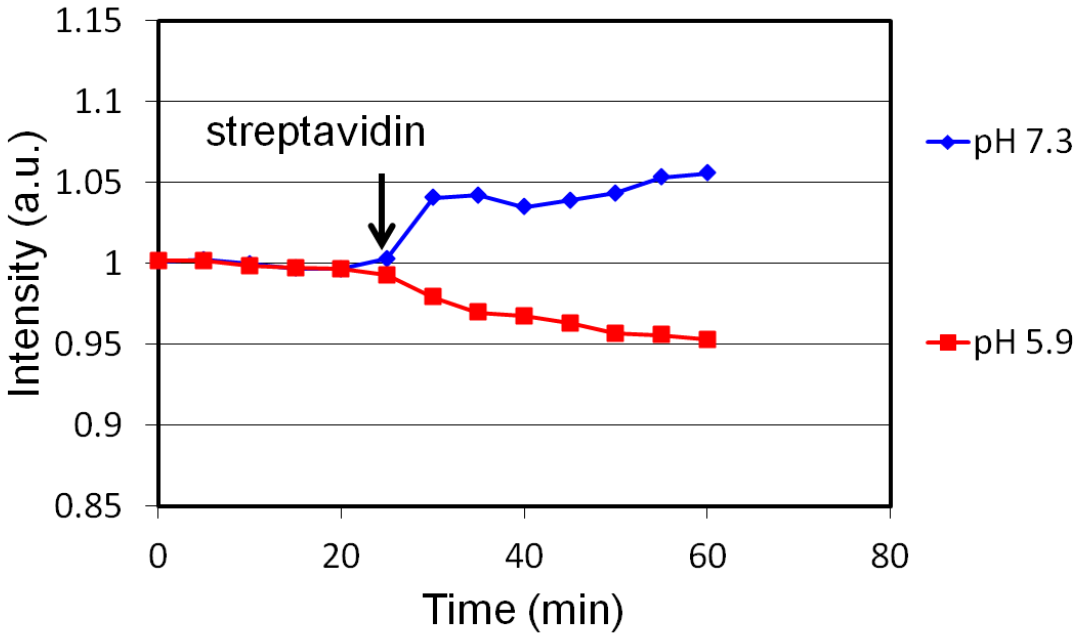


***Figure 3.8.*** Sensing of Streptavidin at Different pH's. Fluorescence intensity measurements before and after the addition of streptavidin at different pH 10 mM PBS 150 mM NaCl buffers. Each point represents the average intensity of a microfluidic channel at a given time.

**Discussion.** Two constraints apply to the sensor that has been described. Firstly, it is necessary that this system operate at pH ranges in which there is a linear response to fluorescence intensity with changing pH. It is also necessary that proteins of interest be sufficiently charged to induce a detectable change in fluorescence upon binding. Through the manipulation of the ionic strength of the operating buffer, it was possible to shift the linear range of the system to higher pH levels and thus increase the operating range of the system, consequently allowing for detection of proteins at pH's adequately far from their pI's. As can be seen from Figure 3.5, a system comprised of POPC, biotin PE, and rhodamine B-POPE operates linearly in a pH range from 5.9 to 7.3. By removing the 150 mM NaCl from the 10 mM PBS operating buffer, this linear range was shifted upwards to pH 8.1, resulting in a shift in apparent pKa for the rhodamine B-POPE of ~1. This results in an average signal upon binding that is three times higher for streptavidin and more than five times higher for avidin. It should be noted that though the bulk pH is well controlled, the hydronium activity near the bilayer surface is affected not only by the buffer, but by the chemistry of the membrane and the solid support as well which results in the measurement of apparent pKa shifts only. While the reduction of ionic strength allows for a shift in the apparent pKa of the dye and consequential operation at higher pH ranges, it also must affect the signal by increasing the area on the bilayer that each protein affects upon binding.

In the case of avidin, operating the assay under a lower ionic strength but at a higher pH, 8.1 instead of 7.3, results in an operating pH that is closer to the protein's isoelectric point. However, the results show that this is a more sensitive assay for this

protein, indicating that at pH ranges sufficiently below (or above) a protein's isoelectric point, the charged state of the protein is positive (or negative) enough to elicit fluorescent response from the dye. The lysines and asparagines in avidin should render this protein sufficiently basic at both pH 7.3 and 8.1, so that it is the effect of decreased ionic strength that enables one condition to be more sensitive that the other. It is therefore important to consider both the operating pH and consequential charge of the protein as well as the Debye length and consequential "footprint" of the binding protein when optimizing this assay for increased overall signal. In the case of streptavidin, when assays were performed with increasing ionic strength but at a constant pH the sensitivity decreased (Figure 3.9) further supporting this idea.

This label-free assay can be utilized to detect the interactions of charged species with a supported lipid bilayer in pH ranges that can be tuned not only through the modulation of the ionic strength of the buffer but through modulation of the buffering species as well as the composition of the bilayer itself. Representative titration curves are shown in Figure 3.10 which detail ortho-rhodamine B-POPE fluorescence response to pH in different buffering conditions and with different bilayer chemistries. Strategic selection of the appropriate combinations of buffer, ionic strength, and surface chemistry affords the ability to tune this assay to conditions that favor the identification of specific membrane-interacting species.

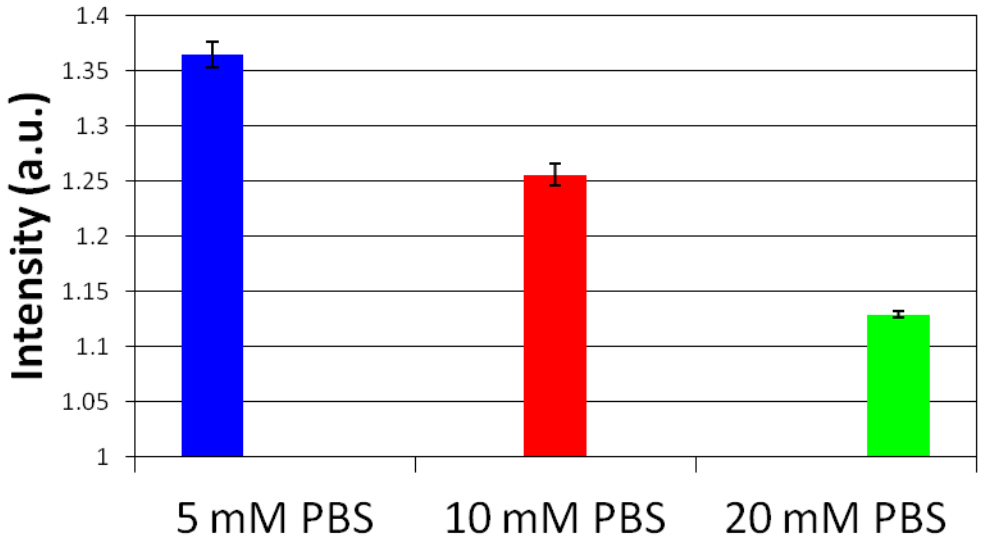


***Figure 3.9.*** Protein Sensing Signal at Different Buffer Concentrations**.** Fluorescence response relative to a starting signal of 1 after addition of 300 nM streptavidin at pH 8.1 in buffers of varying ionic strength. Bilayers consisted of 0.5 mol% *ortho*-rhodamine B-POPE and 5 mol% biotin in POPC. Error bars correspond to standard deviation of multiple fluorescent measurements made on each channel after stabilization.

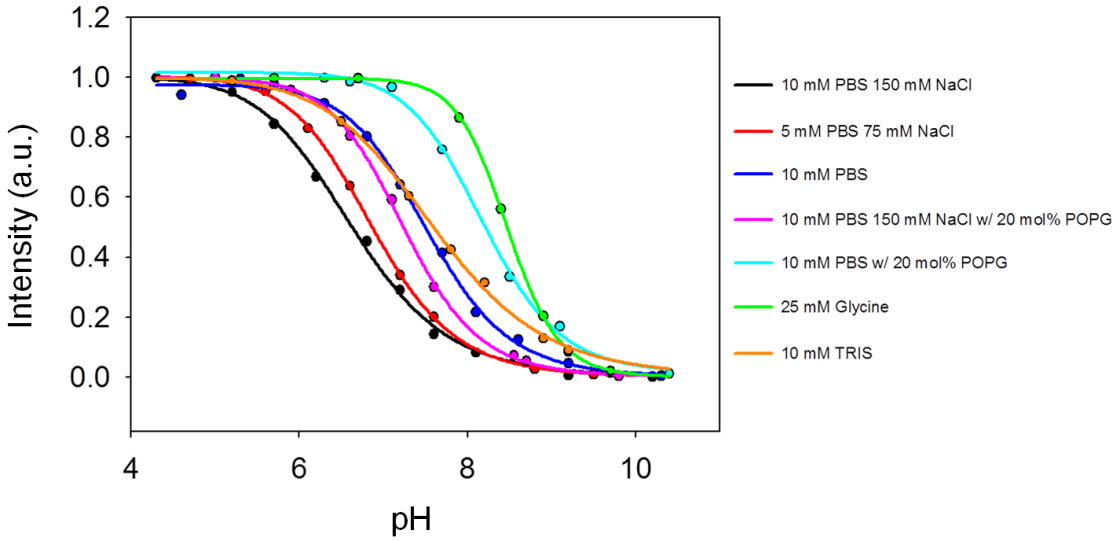


***Figure 3.10.*** pH Titration Curves for Different Buffers and Surface Chemistries.

# CHAPTER IV

# LABEL-FREE MONITORING OF MEMBRANE-ASSOCIATED PEPTIDES ON SUPPORTED LIPID BILAYERS

**Introduction.** The ability to study the interaction between negatively charged phospholipids and basic peptide sequences is appealing for several reasons. Firstly, there exist many proteins which contain amino acid sequences rich in basic residues in their membrane associating regions which facilitate interaction with negatively charged phospholipids such as phosphatidylserine (PS) or phosphatidylglycerol (PG) within plasma membranes. Often these residues are located within the cytoplasmic region of membrane-associated proteins, thereby aiding in the orientation of the protein within the membrane.[78,79] For example, the membrane-spanning glycophorin A, one major human erythrocytic sialoglycoprotein, contains a high percentage of basic residues in its intramembranous region.[80] Membrane-associated proteins also exhibit basic amino acid motifs, a striking example being the myristoylated alanine-rich C kinase substrate (MARCKS) enzyme, the beginning sequence of which is comprised of five consecutive lysine residues.[81,82] Protein kinase C is also believed to utilize basic amino acid lengths in its PS association and subsequent activation.[83] Similarly, many acidic phospholipid-associated cytoplasmic proteins are believed to bind via basic amino acid sequence motifs.[84,85]

Basic amino acid residues are also associated with all classes of antimicrobial peptides.[42] These peptide sequences utilize the electrostatic interaction of positively

charged amino acids with negatively charged bacterial membranes and as such are key in the discriminate defense of zwitterionic eukaryotic cells against invading pathogenic species.[86,87] There is great diversity in describing the mode of operation for antimicrobial peptides, such as barrel stave[88] and toroidal[89] pore formation as means of disrupting microbial membranes, though pore formation is not evident as the means by which most antimicrobial peptides operate.[90] Instead, it appears that the majority of antimicrobial peptides disrupt bacterial membranes via more non-specific interactions. The aptly named carpet model in which peptide accumulation parallel to the membrane can eventually result in a critical concentration and subsequent internalization, resulting in the overall disruption of the bilayer was originally used to describe the membrane permeating behavior of positively charged mammalian cecropins.[91] A more general description of the membrane destabilizing activity of antimicrobial peptides involves the intercalation of peptides into the lipid membrane in a similar manner as detergent molecules infiltrating and ultimately disintegrating bilayers.[92] Regardless of the inherent mechanism associated with antimicrobial activity, the presence of positive amino acid residues remains a constant characteristic of these peptides. With increasing incidence of microbial resistance to drug therapies[93] there exists a pressing need to explore the utilization of antimicrobial peptides as possible therapeutic solutions. The ability to study simplified model peptides may give insight into the nature of antimicrobial membrane association.

Finally, basic residues play a major role in the membrane translocating properties of cell-penetrating peptides (CPP's). One of the main challenges for delivering

therapeutic drugs, specifically those targeted for intracellular organelles such as the mitochondria or nucleus, is transport of these agents across cell membranes.[94] It was originally discovered that tumor cells experienced uptake of albumin facilitated by basic amino acids and histones, especially those containing arginine[95] and after the HIV transactivator of transcription (Tat) protein was shown to be able to permeate cell membranes,[96,97] identification of the active residue sequence which enabled this membrane permeability was accomplished.[98] This multi-arginine and lysine containing sequence, in addition to many other cell penetrating peptides sequences, has been used in the transport of cargos and therapeutics into cells.[99-102] For the majority of CPP's, activity is related to the peptides being composed of multiple arginine and/or lysine residues, and therefore holding a positive charge at physiological pH. Through electrostatic interactions, in addition to potential hydrogen bonding in the case of arginine-containing peptides, association with membrane surfaces can lead to internalization of peptides and their cargo.[94] Therefore, the ability to study the interaction of arginine and lysine-containing peptides with plasma membranes can be useful for insight into this association process and may bring about strategies for delivery of therapeutic cargos into cells.

Indeed, studies involving techniques such as ultrafiltration, dialysis, and electrophoretic mobility measurements have been performed studying the interaction of various lengths of peptides composed of lysine and arginine with negatively charged vesicles.[4,103-105] This, in association with computational modeling,[12] has shed light on the nature of simple cationic peptide association with negatively charged phospholipids.

Because fluorescent labels on these peptide sequences can drastically alter their association properties,[12] it is desirable to monitor their interactions in a label-free manner.

The development of label-free monitoring on supported lipid bilayers via local pH-modulation affords the opportunity to study the interaction of small basic peptides with negative phospholipid membranes in real-time continuous flow. A pH-sensitive dye such as *ortho*-rhodamine B conjugated to a phospholipid is present in a supported lipid bilayer that contains some percentage of PG. When a positively charged peptide such as nona-lysine is introduced and binds to the membrane surface, this will result in modulation the local hydroxide activity. In this case, as *ortho*-rhodamine B loses its fluorescence when deprotonated at higher pH, a decrease in fluorescence of the bilayer will accompany a peptide binding event (Figure 4.1). Thermodynamic data was obtained for sequences of nona-lysine and nona-arginine with supported lipids bilayers containing varying mole percentages of PG and *ortho*-rhodamine B. This approach is unique in its simplicity and ability to provide sequentially built binding isotherms of small basic peptides to supported lipid bilayers and the results confirm the increased affinity of arginine over lysine in PG association as well as increased affinity for bilayers containing a higher mole percentage of PG. Interestingly, the binding isotherms suggest that lysine peptides experience a non-cooperative effect upon binding, which may be attributed to the buildup of positive charge on the bilayer thereby resulting in repulsive electrostatic forces. Arginine, however, shows this non-cooperative effect only at low PG concentrations, suggesting that long-range repulsive effects become outweighed by

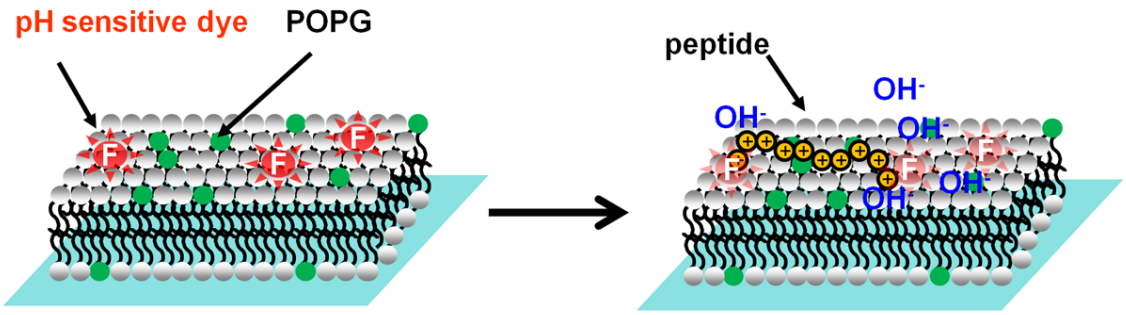


***Figure 4.1.*** Schematic for Peptide Sensing Assay. A supported lipid bilayer containing pH sensitive dye and negative phospholipids (POPG in green) is exposed to positively charged peptide, thereby recruiting hydroxide ions to the membrane surface and deprotonating the fluorescent reporter.

short-range attraction at higher PG concentrations due to the ability of the guanidinium moieties to interact with one another.[106]

**Flow-Cell and pH Titration Curves.** Initially, bilayers containing differing mole percentages of 1-palmitoyl-2-oleoyl-sn-glycero-3-phospho-(1'-rac-glycerol) (sodium salt) (POPG) were prepared utilizing PDMS micro-contact techniques.[58,107] Vesicles containing the appropriate concentration of POPG were incubated in a PDMS well on glass that had previously been stamped with bovine fibrinogen using a PDMS stamp. After a ten minute incubation, the excess vesicles were rinsed away and the flow cell was assembled, allowing for solution to flow over the bilayer formed on the bare glass surface (Figure 4.2). Solutions of 10 mM PBS solution containing 150 mM NaCl were adjusted to specific pH values and flowed into the flow cell. Fluorescence images were taken until the intensity stabilized, and these values were used to form titration curves as seen in Figure 4.3. Data points were normalized to the highest intensity and fit with a sigmoidal curve, from which apparent pKa values were extracted. As can be expected, the apparent pKa of the *ortho*-rhodamine B dye shifts to higher values as the percentage of PG in the bilayer is increased (Table 4.1). This would indicate that with an increasingly negative membrane the bulk pH must be adjusted to higher values to effectively deprotonate the dye at the bilayer surface. There lies within these titration curves a linear range that spans approximately one pH unit and it is within this range that binding measurements are performed.

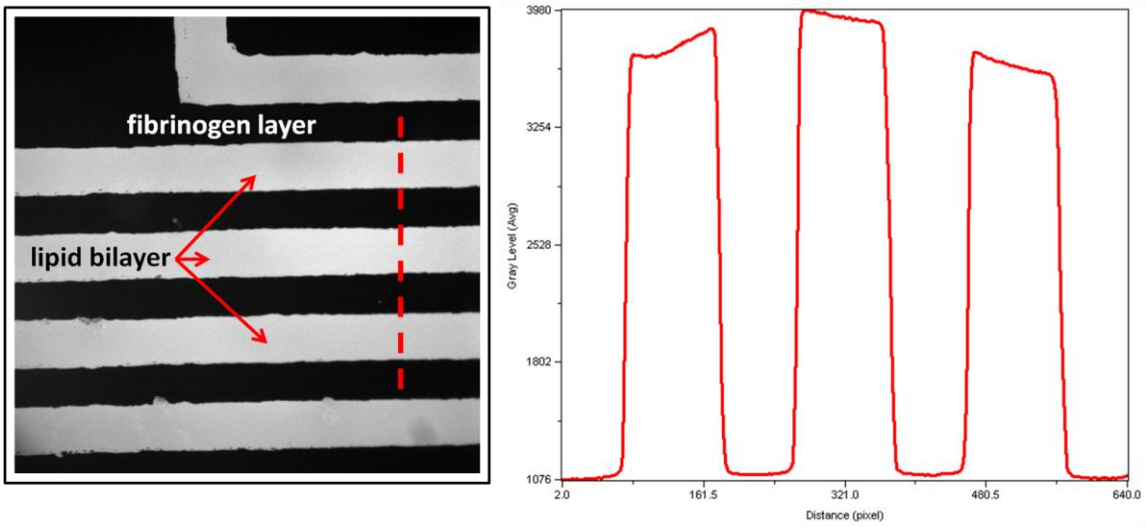


***Figure 4.2.*** Fluorescence Micrograph and Line Scans for Bilayers in Flow Cell. On the left a fluorescence micrograph of supported lipid bilayers containing *ortho*-rhodamine B POPE patterned down on bare glass between fibrinogen-passivated regions. Solution containing different peptide concentrations were flowed over the bilayers, and fluorescence intensity measurements were made accordingly. The line scan on the right shows the fluorescence intensity corresponding to that region marked by the dashed red line in the micrograph.

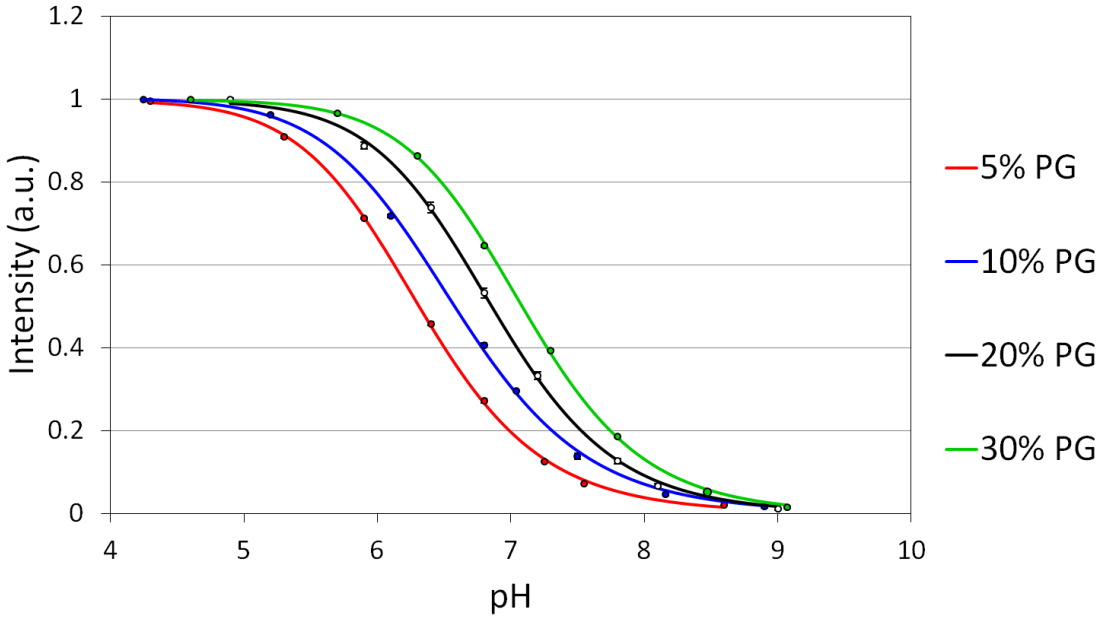


***Figure 4.3.*** pH Titration Curves for Different mol% POPG Bilayers. Titration curves for 5, 10, 20, and 30 mol% POPG bilayers with 0.5 mol% *ortho*-rhodamine B POPE and the remainder POPC. All titration curves were taken with 10 mM PBS with 150 mM NaCl. Apparent pKa values are 6.3, 6.6, 6.9, and 7.3 for 5, 10, 20, and 30 mol% POPG bilayers, respectively.

**Table 4.1.** Summary of Peptide Binding Data for Different PG Concentrations.

| mol% POPG | K9 | | R9 | | app. pKa 10 mM PBS 150 mM NaCl |
|---|---|---|---|---|---|
| | $K_D$(μM) | n | $K_D$(nM) | n | |
| 5 | 77 ± 20* | 0.12* | 460 ± 47 | 0.68 | 6.3 |
| 10 | 55 ± 3 | 0.22 | 124 ± 16 | 0.73 | 6.6 |
| 20 | 2.5 ± 0.5 | 0.24 | 38.5 ± 5 | 1.0 | 6.9 |
| 30 | 2.1 ± 0.8 | 0.19 | 29.3 ± 7 | 1.0 | 7.1 |
| *assay performed at pH 6.4; all others performed at pH 6.8 | | | | | |

**Nona Lysine Binding Experiments.** To monitor the interaction of nona-lysine with the supported lipid bilayer, 10 mM PBS buffer with 150 mM NaCl at a pH of 6.8 was flowed through the flow cell until stabilization of fluorescence intensity occurred. This stabilized fluorescence was recorded with micrographs at five minute intervals, and upon achieving stabilization, the lowest concentration of peptide was suspended in the same buffer and flowed over the bilayer. Micrographs were taken every five minutes until the fluorescence intensity again stabilized, at which time a higher concentration of peptide was introduced. Line scans across the bilayer regions were taken to determine the fluorescence intensity measurements, as shown in Figure 4.2. A graph of the fluorescence intensity values recorded with respect to time, normalized to an initial

intensity of 1, can be seen in Figure 4.4. It is possible to fit a binding isotherm by plotting the negative of the change in fluorescence normalized to the maximum change in fluorescence for the highest peptide concentration added. Interestingly, this plot is not well fit with a single Langmuir isotherm. Instead, it seems to be best fit with a Hill-Waud (eq 4.1) binding model, which is indicative of some form of cooperativity in the binding process. By fitting the data to this isotherm, it is possible to extract equilibrium binding constants:

$$F = F_{max}\frac{([P])^n}{(K_D)^n + ([P])^n} \qquad (4.1)$$

where F is the fluorescence intensity value due to the binding of peptide to the bilayer surface (in this case the negative of the change in fluorescence intensity with respect to a starting intensity of 1), $F_{max}$ is the maximum change in the fluorescence intensity at a peptide concentration that would theoretically saturate the bilayer surface, [P] is the bulk peptide concentration, $K_D$ is the apparent dissociation constant and n is the Hill coefficient of cooperativity. The binding isotherms for nona-lysine interacting with bilayers containing 10, 20, and 30 mol% POPG can be seen in Figure 4.5. These binding isotherms were all conducted at pH 6.8 in 10 mM PBS with 150 mM NaCl. Apparent dissociation constants extracted from these isotherms have values of 55 ± 3, 2.5 ± 0.5, and 2.1 ± 0.8 μM for 10, 20, and 30 mol% PG bilayers, respectively. The Hill-Waud fit for these data sets gives n values that are well below unity, indicating this process experiences negative cooperativity. This may be attributed to the buildup of positively charged peptide at the bilayer surface, which over time may lead to a reversal of the zeta

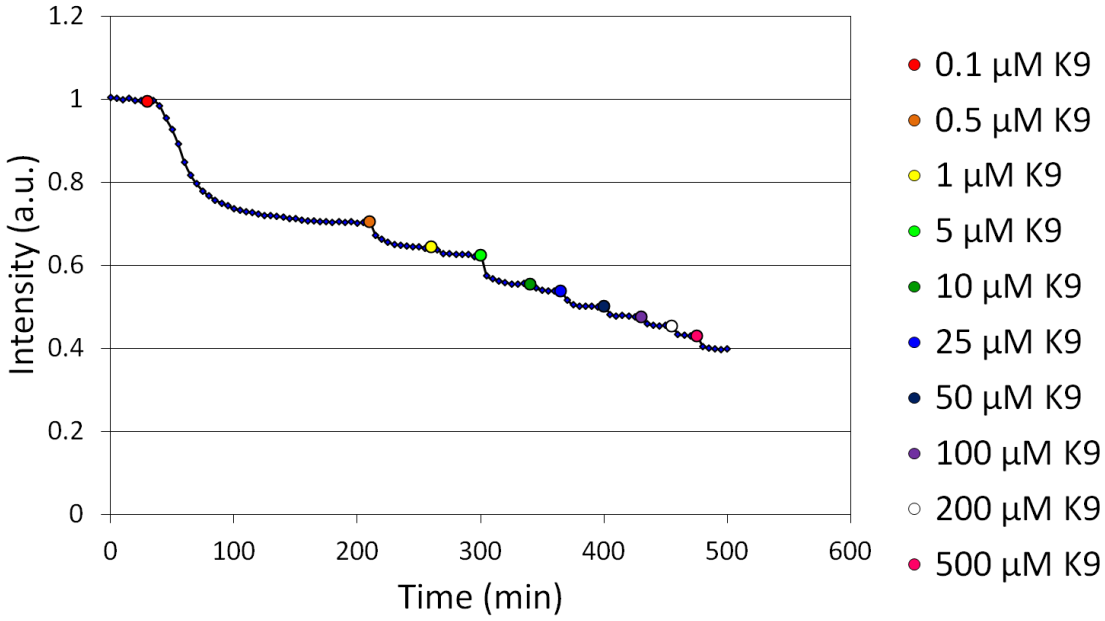


***Figure 4.4.*** Fluorescent Intensity vs. Time for Nona-Lysine Assay**.** Normalized fluorescence intensity measurements for bilayers composed of 0.5 mol% *ortho*-rhodamine B POPE, 30 mol% POPG and 69.5 mol% POPC as increasing concentrations of nona-lysine (K9) peptide is introduced. The buffer used was 10 mM PBS with 150 mM NaCl at pH 6.8.

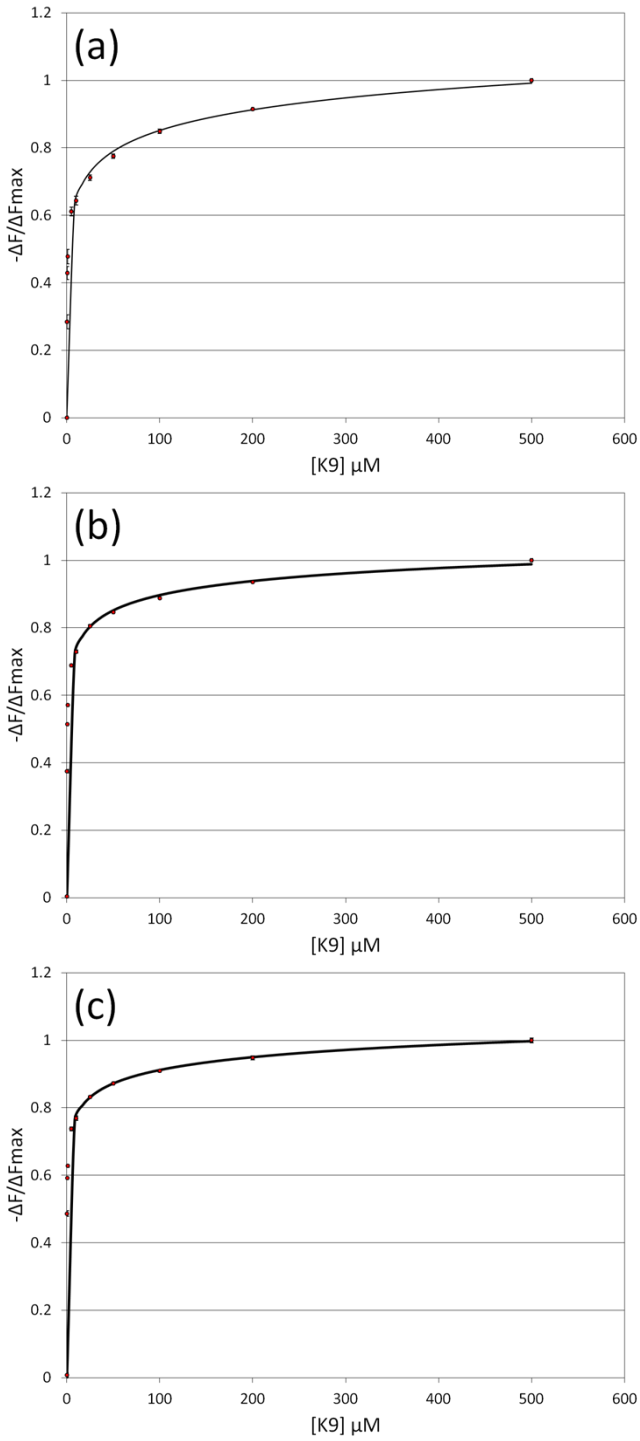


***Figure 4.5.*** Nona Lysine Binding Isotherms for 10, 20, and 30 mol% POPG. Hill-Waud binding isotherms for nona-lysine (K9) associating with a) 10, b) 20 and c) 30 mol% POPG bilayers in 10 mM PBS with 150 mM NaCl at pH 6.8.

potential of the membrane surface. Indeed, it has been reported that vesicles with anionic lipids can experience a reversal of charge upon incubation with high concentration of cationic peptides.[4,12] Unpublished electrophoresis data performed in our laboratory have indicated that this may indeed be the case, as more and more positive peptide accumulates on the bilayer. It is known that poly-lysine will not penetrate beyond the membrane head group region,[104,108,109] suggesting that the electrostatically-driven binding process could experience negative cooperativity as positive charge builds up on the bilayer surface.

It is important to note that this assay may not differentiate between the localized hydroxide activity that is modulated due to a charged peptide binding event and the modulation of bulk solution pH due to high concentration of titratable species, such as nona-lysine. To verify that the fluorescence signal is indeed due to localized binding events, control experiments were run with bilayers containing 0.5 mol% *ortho*-rhodamine B POPE and POPC with high concentrations of nona-lysine. In this case, no peptide should associate with the bilayer surface and any modulation in fluorescence intensity should be due to bulk pH fluctuation. As can be seen in Figure 4.6, even at the highest concentration of nona-lysine utilized in these experiments, there is little discernible change in the fluorescence intensity, suggesting that measured signal is indeed due to direct association of the peptide with the bilayer surface.

An additional nona-lysine experiment was performed on bilayers composed of 0.5 mol% *ortho*-rhodamine B POPE, 5 mol% POPG and POPC. In this case, the assay was run at a pH of 6.4 as opposed to 6.8. The binding isotherm again shows a best fit to

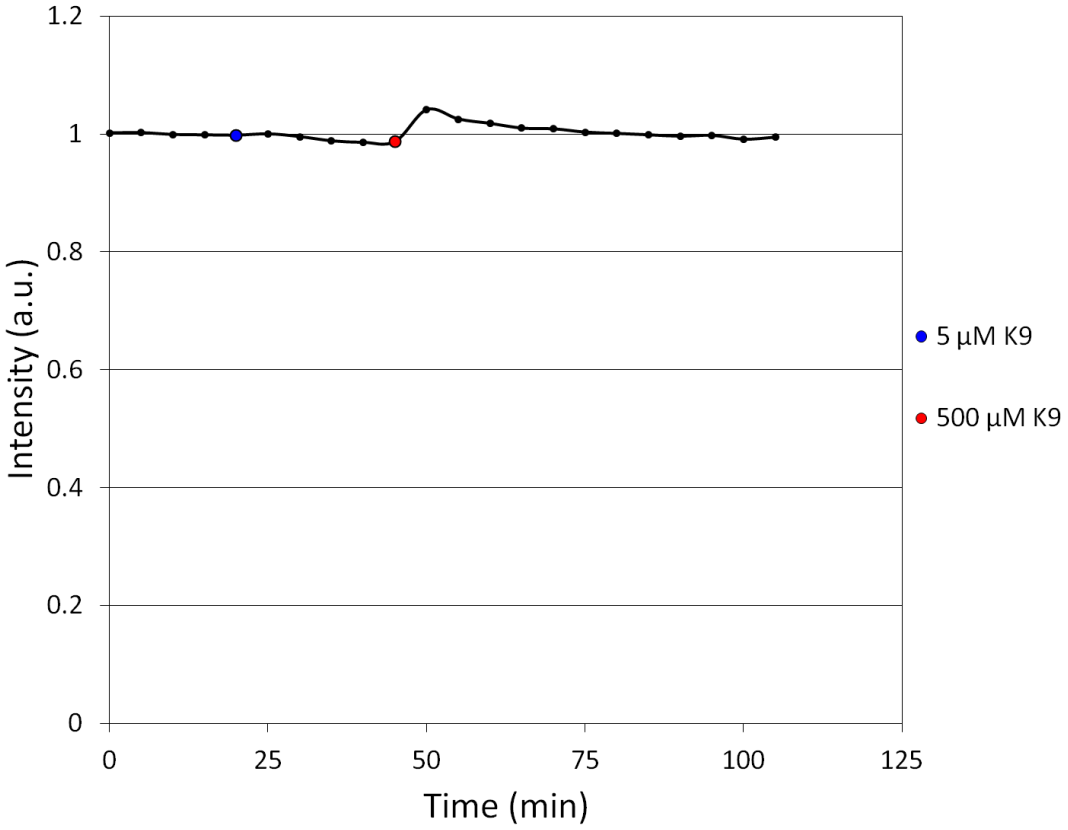


***Figure 4.6.*** Control Assay with POPC Bilayer**.** Control experiment showing fluorescence intensity measurements for a bilayer composed of 0.5 mol% *ortho*-rhodamine B POPE and POPC. The colored points indicate times at which increasing concentrations of nona-lysine were added, revealing that the bulk pH is not being modulated by the addition of peptide.

the Hill-Waud model with negative cooperativity with an apparent $K_D$ value of 77 ± 20 μM (Figure 4.7). As the pH is lowered, one would expect the possibility of having a more positively charged peptide in the case of nona-lysine. It is known that decreasing the ionic strength results in stronger binding for these systems,[4] suggesting that modulating the charged state of the peptide could increase the binding affinity to anionic bilayers. This should be taken into account when viewing the Hill coefficients for these four bilayer systems (Table 4.1), as a 5 mol% PG bilayer would seemingly give rise to less negative cooperativity due to a decreased binding density on the bilayer surface.

**Nona Arginine Binding Experiments.** Experiments were then performed wherein varying concentrations of nona-arginine peptide were flowed over supported lipid bilayers of varying POPG concentrations in a flow cell device. In a similar manner, decreased fluorescence of the bilayer was observed for increasing concentrations of nona-arginine and plotting the negative of the change in fluorescence relative to the change in fluorescence of the highest concentration of peptide added allows for the formulation of binding isotherms (Figure 4.8). These assays were performed in 10 mM PBS with 150 mM NaCl at a pH of 6.8. Comparison of the apparent Kd values for the nona-arginine with the nona-lysine confirms the higher affinity of these poly-arginine peptides for anionic phospholipid bilayers (Table 4.1). As for the nona-lysine peptide, both 5 and 10 mol% POPG bilayers give fluorescence response signals that are best fit to a Hill-Waud isotherm showing negative cooperativity with Hill values less than unity. As can be seen in Table 4.1, the Hill coefficient values are much closer to unity than

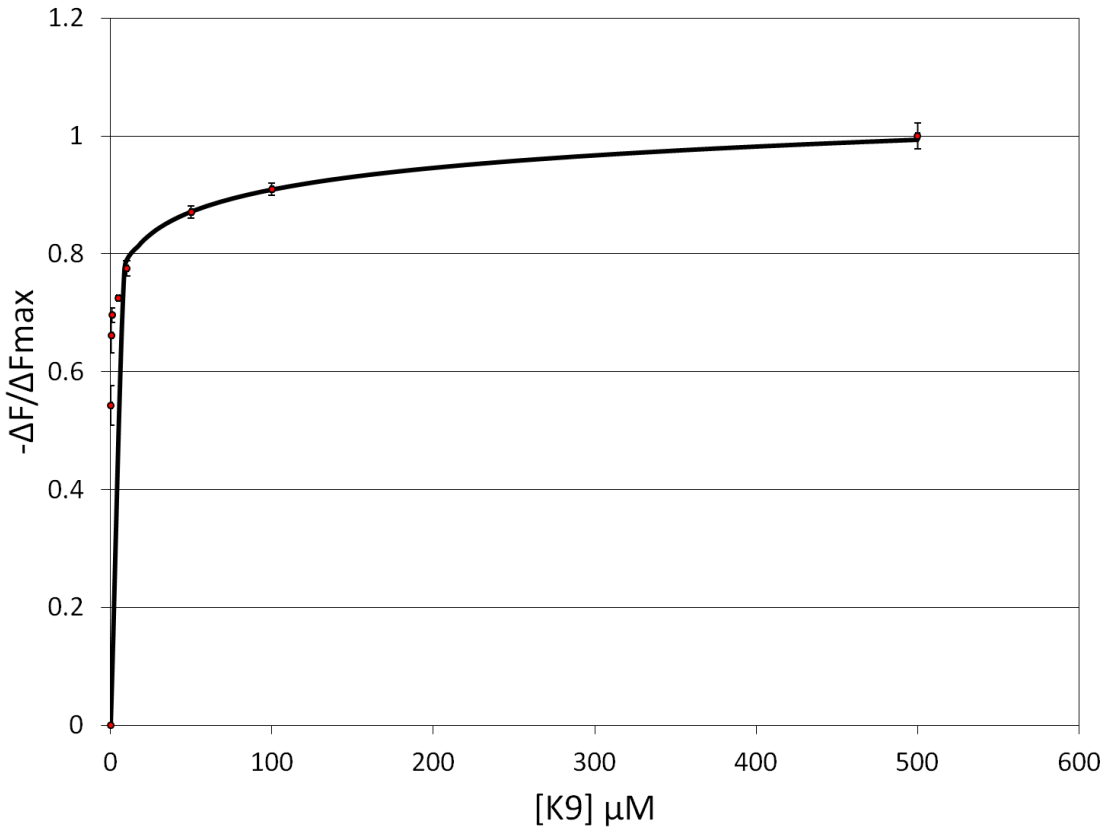


***Figure 4.7.*** Nona Lysine Binding Isotherm for 5 mol% POPG**.** Hill-Waud fit to fluorescence intensity measurements for bilayers composed of 0.5 mol% *ortho*-rhodamine B POPE, 5 mol% POPG, 94.5 mol% POPC with the addition of nona-lysine (K9) in 10 mM PBS with 150 mM NaCl at pH 6.4.

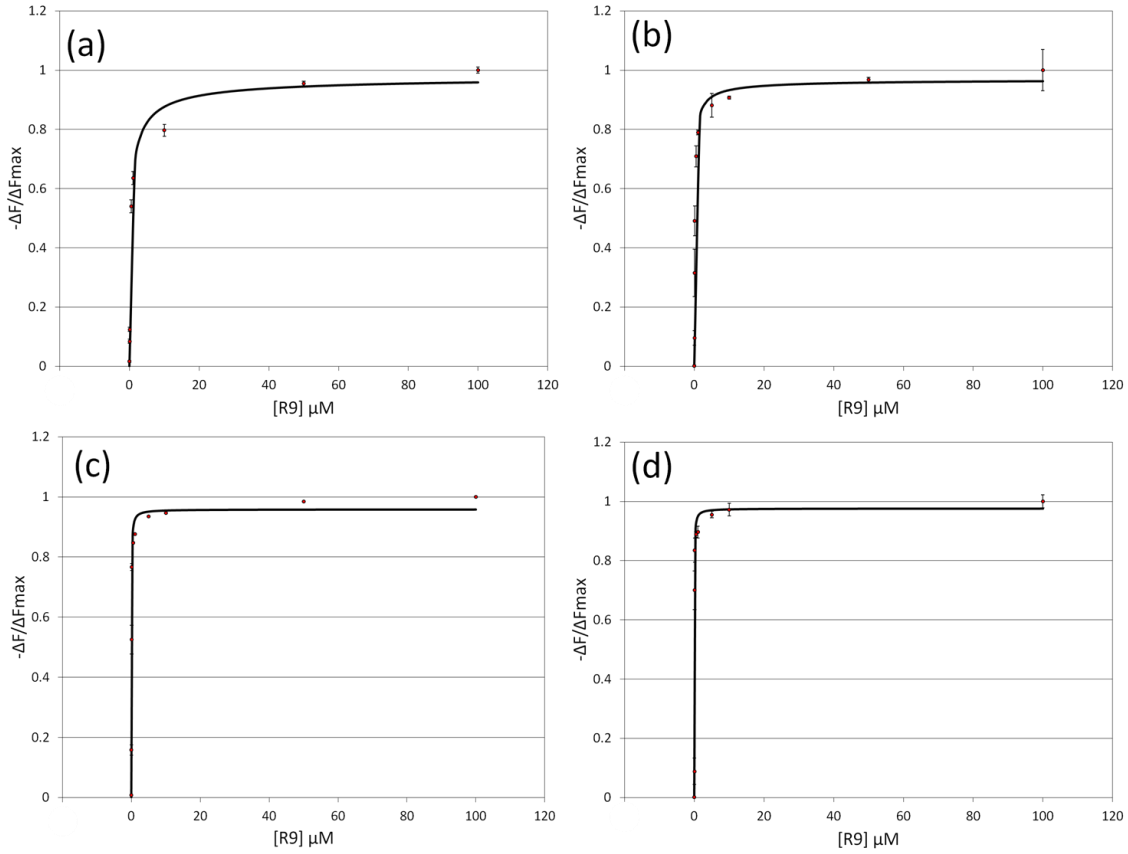


***Figure 4.8.*** Nona Arginine Binding Isotherms**.** Binding isotherms for nona-arginine peptide associating with a) 5, b) 10, c) 20 and d) 30 mol% POPG. All measurements were made in 10 mM PBS with 150 mM NaCl at pH 6.8.

those values calculated for nona-lysine binding. In addition, the bilayers composed of 20 and 30 mol% POPG are best fit with Hill coefficients of one, suggesting non-cooperativity in which a traditional Langmuir isotherm accurately describes the fitting.

**Discussion.** The structural make up of nona-lysine and nona-arginine peptides is similar in many ways. Both of these peptides are highly positively charged and are well known to associate with anionic phospholipids, especially phosphatidylglycerol and phosphatidylserine.[4] However, polypeptides of these two amino acids show very different behavior, both in the strength and mode of their interaction. It has been shown that lysine, although associated with cell-penetrating peptide sequences such as the TAT domain of HIV, does not show propensity to translocate membranes to become internalized as a homogenous polypeptide.[110] Arginine has been shown to not only improve the membrane-penetrating capacity of polypeptide sequences such as the TAT domain of HIV when it is substituted in place of the inherent lysine residues,[111] but exhibits membrane-translocating behavior as a homogeneous polypeptide as well.[112] The difference in behavior between these two amino acids must lie in the nature of their cationic moieties.

Lysine, with an ammonium group comprising its charged moiety, can be expected to interact predominately via electrostatic effects. The technique presented here affords the ability to monitor the interaction of nona-lysine peptides with supported lipid bilayers containing various concentrations of PG in a label-free manner while extracting thermodynamic spectroscopic data. It is interesting that the binding isotherms do not

show single Kd Langmuir isotherm binding behavior but instead are well fit by Hill-Waud isotherms. Indeed, the thermodynamic data herein suggests that these peptides experience negative cooperativity in their binding to PG-containing bilayers as is suggested by Hill coefficients significantly below unity. This negative cooperativity may be attributed to the gradual reversal of the potential of the membrane surface as lysine peptide begins to populate the head group region. In a monovalent salt solution such as is the case here, the surface potential ($\psi_0$)can be related to the surface charge density ($\sigma_0$) by the Graeme equation:

$$\sigma_0 = \sqrt{8\epsilon_0\epsilon kT[Na^+]}\sinh\left(\frac{e\psi_0}{2kT}\right)$$

where $\epsilon_0$ is the permittivity of a vacuum, $\epsilon$ is the relative permittivity of water, k is the Boltzmann constant, e is the magnitude of electronic charge and T is the temperature. When $|\psi_{(0)}|$ is < 25 mV, this can be reduced to

$$\psi_0 = \frac{\sigma_0}{(\epsilon_0\epsilon\kappa)}$$

showing that the surface potential is proportional to the surface charge density under these conditions. As nona-lysine residues begin to populate the surface, each peptide is predicted to bind up to eight PG lipids,[4] with the result being a reversal of surface charge density and therefore surface potential. The reversal of charge on PG vesicles has been shown with penta-lysine[4] and electrophoretic results in our laboratory have also suggested that the membrane potential can be reversed upon peptide binding. In light of

this, negative cooperativity seems justified and should be exacerbated upon higher PG concentrations.

For the binding of poly-arginine peptides, the situation is slightly more complicated, and can be attributed to the guanidinium present as the cationic moiety. In addition to purely electrostatic interactions, arginine is believed to experience some non-electrostatic interaction mechanisms such as hydrogen bonding, which has been attributed to interactions of arginine with phospholipids.[113] Although arginine residues are highly charged, there is evidence that they may overcome typical like-charge repulsion with the capacity for pairing such as is found in some protein structures.[114,115] Guanidinium ions have been shown to form parallel stacks in solution,[116] and computational work done with molecular dynamics and *ab initio* calculations has confirmed the ability of guanidinium pairing in arginine-rich peptides as well as in solution.[106] The ability for the guanidinium moiety in poly-arginine peptides to experience close-range attraction due to its capacity to form parallel stacks helps to explain the trend that is observed in the binding isotherms for nona-arginine peptides in this study. Hill-Waud fits to the thermodynamic data show a trend in the Hill coefficient wherein the binding of nona-arginine experiences less negative cooperativity as the concentration of PG in the bilayer increases, with the higher concentrations showing a best fit with a Hill coefficient of one.

Guanidinium, being a planar ion, has the ability to form in-plane hydrogen bonds upon binding to anionic membranes. Likewise, these peptides show tighter binding behavior than the purely electrostatic poly lysine, as can be seen from the apparent Kd

values. The parallel stacking that can lead to like-charge association between guanidinium ions occurs on the weakly hydrated face of the ion. With increased concentration of PG in the bilayer, one would expect this close range interaction to begin to dominate the long-range electrostatic repulsion between guanidinium moieties on poly arginine peptides, as is manifested in the Hill coefficient trend for this system.

The studies herein may be extended to observing the interaction of these peptide sequences with different anionic phospholipids, such as phosphatidylserine, and the effect of such additives as cholesterol. In addition to offering some thermodynamic insight into the differences in binding modes of poly lysine and arginine peptides, this simple label-free assay by be extended in its general use as a potential screen for basic peptide sequences associating with anionic membranes in general. With the utilization of multiplexed microfluidic devices, apparent dissociation constants for multiple peptide sequences may be determined simultaneously, while avoiding the cost and perturbation of fluorescent labels.

# CHAPTER V

# LABEL-FREE MONITORING OF PROTEIN-PHOSPHATIDYLSERINE INTERACTIONS ON SUPPORTED LIPID BILAYERS

**Introduction.** Phosphatidylserine (PS) constitutes the most prevalent negatively charged phospholipid species in eukaryotic cells and as such is involved with many important signaling processes as well as recruitment and activation of enzymes. PS is the key phospholipid signaler that is recognized by macrophages in the process of clearing apoptotic cells.[117] Distribution of PS in cell membrane leaflets is highly asymmetrical, with the majority being located in the inner leaflet and thus maintained by the action of flippase enzymes and it is believed that inhibition of this enzyme coupled with the activity of scramblase enzymes contribute to reversal of PS distribution,[118] along with lysosome fusion-mediated redistribution.[119] The presentation of PS on the extracellular membrane is vital in such processes as the coagulation cascade in hemostasis processes.[120] Coagulation proteins such as coagulation factor V and prothrombin recognize the PS headgroup specifically, though with different structural features in their binding domains.[121,122] The function of intracellular PS is also associated with protein binding and function as well, serving as the target for species such as protein kinase C (PKC), which is activated upon binding.

Among the various protein domains associated with PS-binding there exists a range of specificity from general anionic-phospholipid binding regions rich in cationic residues to more PS-specific C2 domains. The mode of traditional PKC binding to PS

involves such a domain. The C2 region recognizes and binds PS via a calcium-dependent interaction, whereby the protein undergoes structural alteration and is consequently activated.[47] Traditional PKC, which includes isoforms α, βI, βII, and γ, is regulated by diacylglycerol in addition to this calcium-mediated interaction with PS. It is the C2 domain, containing specific $Ca^{2+}$ binding regions, which is key in maintaining the enzyme in a bound state with phospholipid membranes.[123,124] The C2 domain is also of considerable interest due to its structural feature, which contains two loops by which calcium is coordinated and PS binding facilitated. These loops have been shown to have bound $Ca^{2+}$ displaced by $Pb^{2+}$ in the presence of PS lipid membranes, suggesting one potential molecular manifestation of well-known but little-understood Pb toxicity.[48]

Recently, we have discovered that PS can bind $Cu^{2+}$ with extremely high affinity in a 2:1 PS:$Cu^{2+}$ complex, a phenomena that is accompanied in bilayers by the quenching of nearby fluorescently labeled phospholipids.[49] This process is reversible and de-quenching can be facilitated by lowering the pH of the solution causing the consequential protonation of the PS molecules. The concentration of $Cu^{2+}$ that is necessary for this quenching to occur is also impressively low, with the equilibrium dissociation constant being in the femtomolar range. In fact, the extremely high affinity of this interaction and its obvious fluorescent response has brought to light the ubiquitous nature of trace $Cu^{2+}$ contamination in buffers, water sources, and various laboratory products such as polytetrafluoroethylene tubing. Without the implementation of PS and fluorescently-tagged phospholipid bilayers, the presence of these $Cu^{2+}$ ions might not have been recognized. This observation presents the possibility that numerous

PS studies, especially those performed in membranes, may be performed in the presence of this strongly associating complex. Herein we describe the utilization of this PS-$Cu^{2+}$ induced quenching as a mode for detecting the C2 PS-binding domain of protein kinase Cα (C2α). This strategy involves the formulation of supported lipid bilayers in microfluidic channels composed of 1,2-dioleoyl-sn-glycero-3-phospho-L-serine (sodium salt) (DOPS), 1-palmitoyl-2-oleoyl-sn-glycero-3-phosphocholine (POPC), and fluorescently labeled 1-hexadecanoyl-2-(9Z-octadecenoyl)-sn-glycero-3-phosphoethanolamine) (POPE). Initially, buffer containing μM concentrations of $CaCl_2$ and nM concentrations of $CuCl_2$ is flown over the bilayers, resulting in the PS-$Cu^{2+}$ quenching of phospholipid-linked fluorophores, in this case the pH-insensitive *para* isomer of rhodamine B. This quenched state is then disrupted by then introducing varying concentrations of C2α, which disrupts the $Cu^{2+}$ ion-induced quenching and results in a turn-on fluorescent response (Figure 5.1). It is possible to elucidate binding isotherms from this fluorescent data, which yield dissociation constants that agree very well with published values for this system.

**C2α Binding Experiments.** Initially, vesicles composed of 0.5 mol% *para*-rhodamine B, 20 mol% DOPS and 79.5 mol% POPC were created. *Para*-rhodamine B, unlike the *ortho* isomer, is pH insensitive and therefore should not fluctuate intensity due to any perturbation of the hydroxide activity a charged protein may induce at the membrane surface upon binding. Instead, the fluorescent signal should come directly

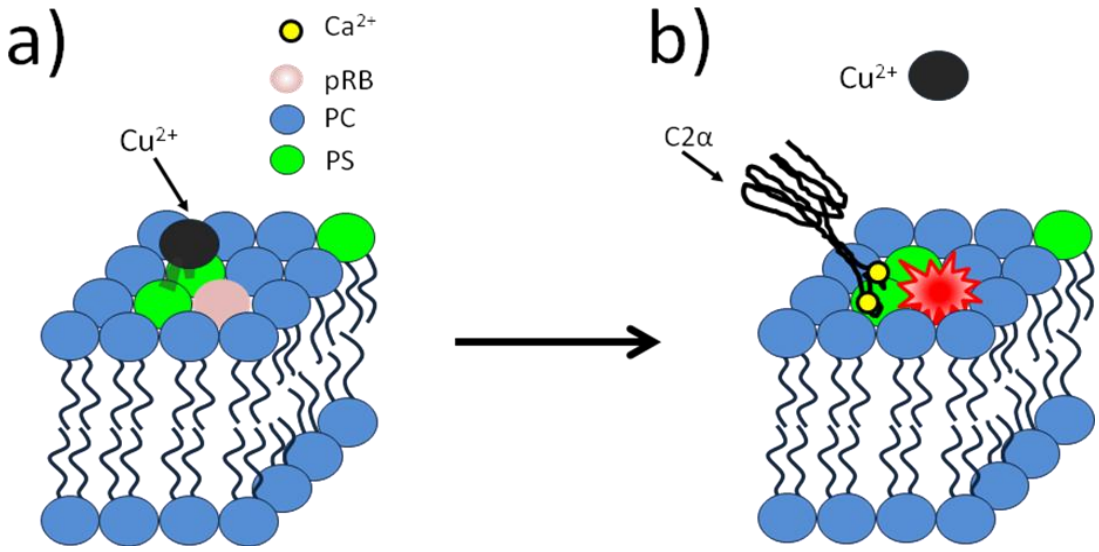


***Figure 5.1.*** Schematic of PS-$Cu^{2+}$ Sensing Assay. Initially a bilayer containing POPC, DOPS, and *para*-rhodamine B POPE (pRB) is in equilibrium with $Cu^{2+}$ in solution with much of the fluorophore in a quenched state (a). Upon the addition of $Ca^{2+}$ complexed C2α, the PS-$Cu^{2+}$ complex is disrupted, consequently de-quenching the dye and increasing the fluorescence intensity of the bilayer (b).

from the disruption of the 2 PS-$Cu^{2+}$-induced quenched state that has initially been established. After introducing vesicles into the microfluidic channels and allowing them to incubate for 30 minutes, 10 mM MES buffer with 100 mM KCl, 100 μM $CaCl_2$, and 1 nM $CuCl_2$ at pH 6.1 was flown through the device. Fluorescence micrographs were taken at regular intervals until fluorescence stabilization occurred. Line scans were taken across the microfluidic channels and measurements were made by averaging the intensity of the middle third of each channel, corresponding to the bilayer most uninfluenced by channel edge effects. As can be seen in Figure 5.2, the intensity begins dropping drastically as the $Cu^{2+}$-induced quenching occurs. For this copper concentration at this pH and flow rate, this process takes approximately one hour to equilibrate, resulting in a fluorescence intensity that is about 20% of the initial unquenched state. This low rate of quenching is indicative of the necessity to form the two-lipid complex with the ion, which depends upon the diffusion of PS in the bilayer.[49] This process can be reversed by either modulating the pH of the solution to much lower values to achieve protonation of the PS or by adding some chelating agent, such as ethelenediaminetetraacetic acid (EDTA) or mM concentrations of glycine. This quenching phenomena can also be disrupted by the addition of the peripheral membrane binding C2 domain of protein kinase Cα (C2α). As can be seen in Figure 5.2, the addition of 50 nM C2α results in a de-quenching process as the 2 PS-$Cu^{2+}$ complex is disrupted by the formation of the $Ca^{2+}$-mediated C2α-PS complex. This process takes several hours to equilibrate and indeed is dependent upon the concentration of $Cu^{2+}$ in solution. At higher copper concentrations, in the 100's of nM, the de-quenching of the

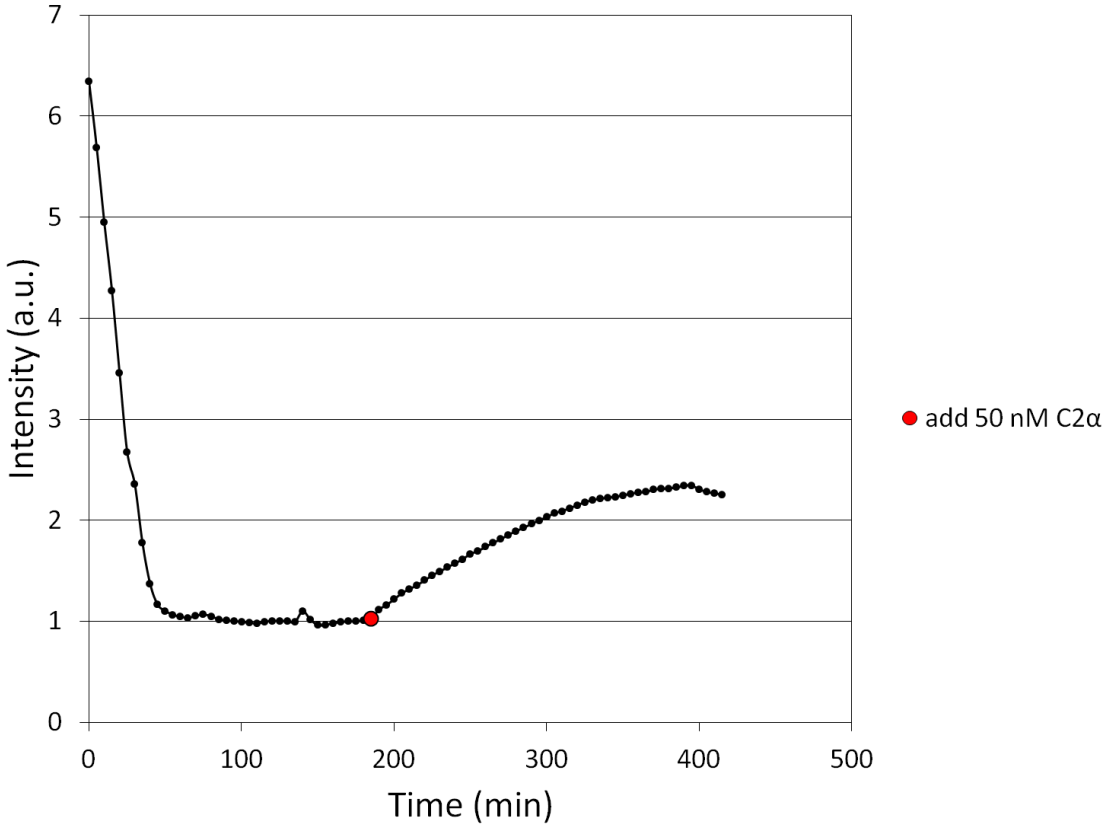


***Figure 5.2.*** Fluorescence Intensity Data for $Cu^{2+}$ Quenching and De-quenching. Fluorescence intensity measurements for a bilayer in a microfluidic channel consisting of 0.5 mol% *para*-rhodamine B, 20 mol% DOPS, and 79.5 mol% POPC. 10 mM MES buffer containing 100 mM KCl, 100 μM $CaCl_2$ and 1 nM $CuCl_2$ was flown into the channel until fluorescence intensity stabilized, at which point 50 nM C2α was added in the same buffer.

fluorophore does not occur with the addition of C2α unless higher concentrations of the protein are added, indicating of a direct competition for PS-binding.

This process was repeated across multiple channels in microfluidic devices to establish a binding curve for C2α in the presence of 100 μM $CaCl_2$. Figure 5.3 shows the line scans for four microfluidic channels in which the bilayers have been first equilibrated with 1 nM $Cu^{2+}$ in a quenched fluorescence state, and then in an equilibrated state after the addition of 500, 100, 10, and 0.5 nM C2α. Figure 5.4 shows the fluorescence intensity data for multiple channels as a function of time with the addition of various concentrations of C2α. One can see that the rate of de-quenching is somewhat varied between concentrations, which can be attributed to the difference in flow rate between different microfluidic channels. This data can be fit with a simple Langmuir isotherm:

$$F = F_{max}\frac{C}{Kd + C}$$

where F is the change in fluorescence intensity due to C2α-induced de-quenching normalized to a maximum change in fluorescence $F_{max}$, C is the concentration of C2α in bulk solution and $K_d$ is the apparent dissociation constant. This isotherm fitting (Figure 5.5) gives an apparent $K_d$ value of 75 ± 8 nM, which agrees well with previously reported values determined by surface plasmon resonance.[48,125] It is important to note that in the absence of any intentional $CaCl_2$, the addition of C2α also showed some de-

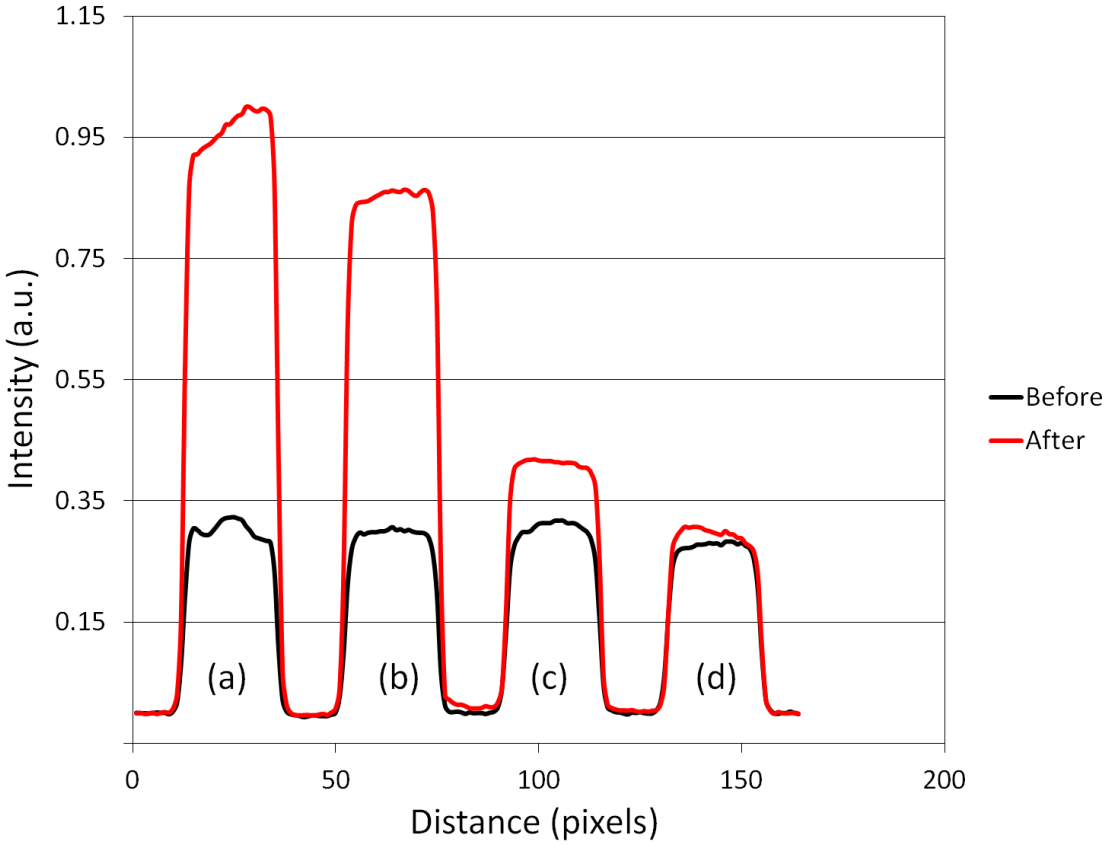


***Figure 5.3.*** Line Scans for C2α Sensing Assay. Line scans for microfluidic channels containing bilayers composed of 0.5 mol% *para*-rhodamine B, 20 mol% DOPS and 79.5 mol% POPC. Fluorescence intensity was equilibrated in 10 mM MES buffer with 100 mM KCl, 100 µM $CaCl_2$, and 1 nM $CuCl_2$ (black line). Fluorescence intensity increased and stabilized (red line) after the addition of a) 500 b) 100 c) 10, and d) 0.5 nM C2α.

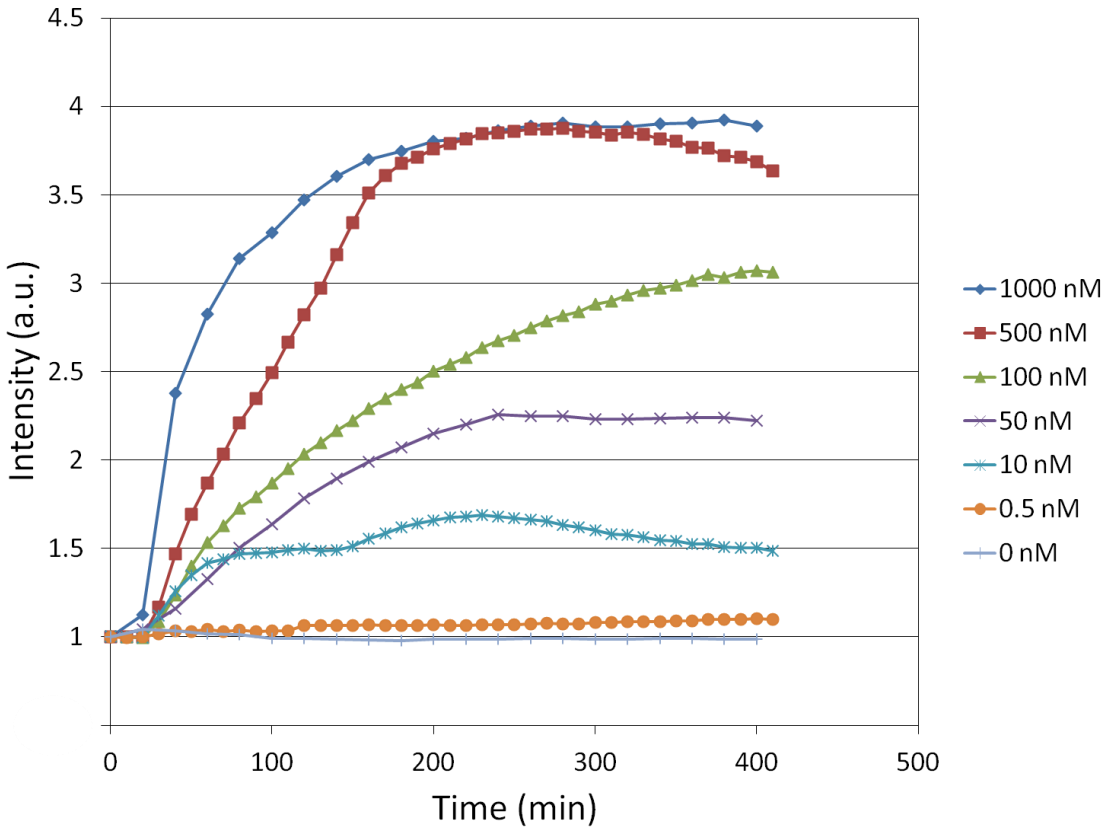


***Figure 5.4.*** Fluorescence Intensity Data for C2α Sensing Assay. Fluorescent intensity measurements versus time for microfluidic channels containing bilayers composed of 0.5 mol% *para*-rhodamine B, 20 mol% DOPS and 79.5 mol% POPC. Differing concentrations of C2α were flown in a buffer consisting of 10 mM MES with 100 mM KCl, 100 µM $CaCl_2$ and 1 nM $CuCl_2$.

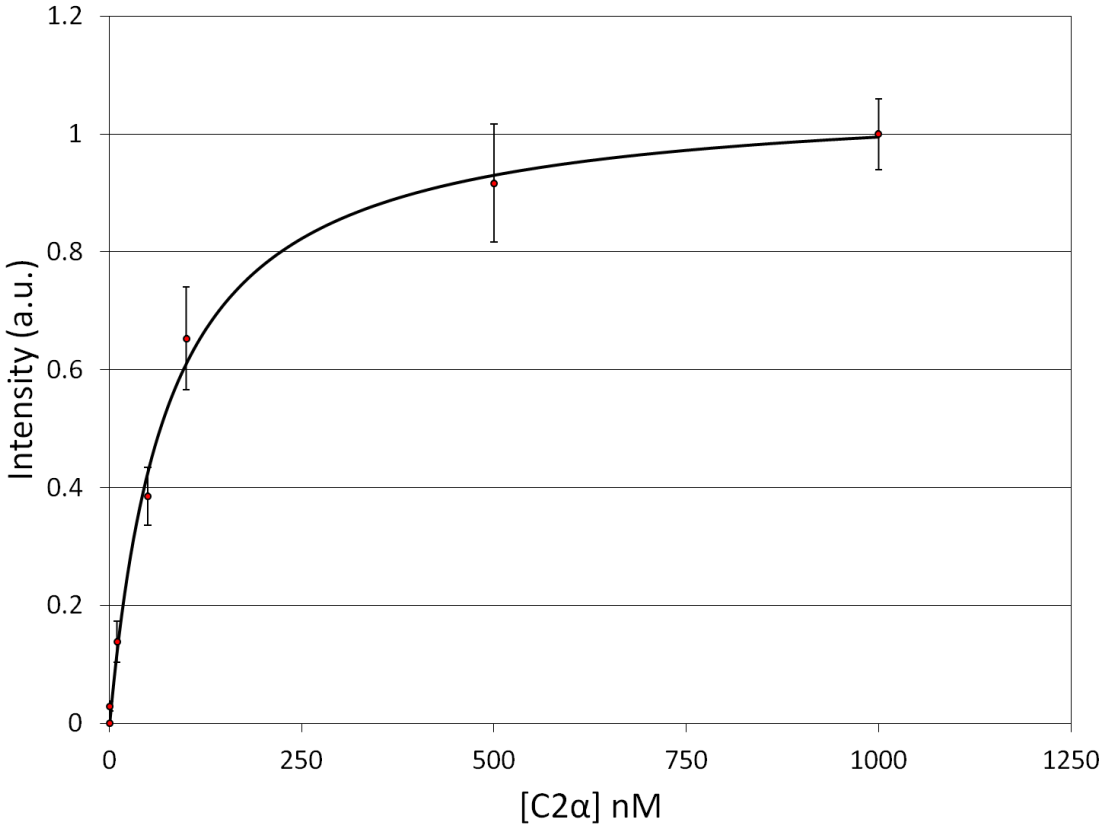


***Figure 5.5.*** Binding Isotherm for C2α. Langmuir isotherm fit to the fluorescence intensity change upon addition of C2α to bilayers composed of 0.5 mol% *para*-rhodamine B POPE, 20 mol% DOPS, and 79 mol% POPC in10 mM MES with 100 mM KCl, 100 µM $CaCl_2$ and 1 nM $CuCl_2$.

quenching of the bilayer fluorescence, though to a lesser extent that in the presence of calcium. NMR data can reveal if $Cu^{2+}$ can be bound by C2α in a similar manner to $Ca^{2+}$, which would explain the dequenching observed upon addition of C2α in the absence of calcium. These studies are ongoing.

**Discussion.** The data presented herein leads to some interesting implications. Firstly, as PS concentrations *in vivo* are estimated to be in the micromolar to low millimolar[43] range and involved in numerous signaling cascades, and considering the high affinity[49] that PS has shown to bind $Cu^{2+}$, it is possible that competition for PS binding may be occurring with such proteins as PKC. This work has demonstrated that the disruption of the two-serine mediated $Cu^{2+}$ bound complex is possible via the introduction of the PS-binding C2 domain of PKC with no apparent affect on the observed dissociation constants for this species in the presence of calcium. This is an interesting disruption to occur, as it involves two different ions which interact differently with PS. Whereas the calcium ion is bound in conjuncture with the phosphate group, the copper ion is held between two serine residues of neighboring PS molecules. It was shown that $Ca^{2+}$ alone can to some extent displace $Cu^{2+}$ and lead to de-quenching, though it must be present in great excess.[49] However, in the case of C2α, there was evidence of de-quenching at concentrations comparable to bulk $Cu^{2+}$.

The high affinity that $Cu^{2+}$ has for PS may be evidence that this phospholipid plays some role in sequestering any free $Cu^{2+}$ that may be present in the cell. If PS is indeed involved in sequestering free $Cu^{2+}$ and neutralizing these toxic species,[126,127] it

may be that this function does not significantly disrupt the role this phospholipid plays as an activator in signaling pathways for cell proliferation and differentiation, such as those is mediated by PKC.[128] Although at high $Cu^{2+}$ concentrations (above 50 nM) there seems to be no de-quenching effect upon addition of C2α, indicating that at this concentration there is no significant C2α binding to PS, in a cell free copper ion concentration is believed to be extremely low,[129] with the majority that is present for enzymatic function in $Cu^{+}$ form.[126]

Another implication is in the technique itself. It would follow that this strategy may be useful to observe in a label-free manner many classes of PS-binding proteins such as annexin V or prothrombin. In addition to the large signal that is generated and its relative simplicity, this assay strategy affords the ability to discover the effect that $Cu^{2+}$ may have on the PS-binding behavior of these proteins, gaining insight into this bio-metallic system.

It is worth noting that in addition to the strategy presented here, binding of C2α to PS was also observed utilizing a pH-sensitive fluorophore, though the signal to noise was not as high as for the $Cu^{2+}$ de-quenching assay.

# CHAPTER VI

# CONCLUSIONS

**Discussion.** The focus of this research has been the exploration and development of label-free fluorescence-based sensors utilizing supported lipid bilayers. The advantages of this strategy include its simplicity of implementation, its adaptation to biologically relevant studies, the fact that it is easily amenable to multiplexing in microfluidic devices, and perhaps most importantly the ability to monitor analytes in a label-free manner. Herein, with the use of supported lipid bilayers, this technique is operated in a heterogeneous manner. However, it is possible and has been shown that this strategy is amenable to homogeneous systems as well.[130] In this manifestation, wherein a protein is fluorescently labeled with a pH-sensitive dye, the interaction with its binding partner can be monitored and binding isotherms can be extracted. This strategy has shown to be able to detect protein-protein, protein-small molecule, and protein-ion interactions in bulk solution. Considering the simplicity of operation and the variety of interactions it is capable of accurately monitoring, this technique seems to be a choice strategy for use in initial screening assays, where a wide variety of targets, such as drugs or peptides, can be run simultaneously allowing for the most promising candidates to be isolated for more in-depth analysis and study.

As with any technique, the label-free sensing strategies presented herein have their inherent limitations. Assays utilizing the pH-modulation approach must involve the detection of a charged species, and the operating pH range should be confined to that

region of linear response from the reporter fluorophore. This is a facet that must be taken into consideration when considering this strategy, although it has been shown that these ranges can be modulated by altering buffer conditions, reporter dyes, or bilayer chemistries. For the utilization of the PS-$Cu^{2+}$ sensing approach the obvious limitation is inherent to the inclusion of these two species. Ultimately, as with any technique, one must identify those candidates which are most amenable to the advantages that a particular strategy affords. The opportunity to collaborate with both the Pellois laboratory for the peptide studies presented and the Igumenova laboratory for the C2α investigations has proven to be helpful in discovering specific applications for these sensing strategies that have interesting biological implications. The future of this work lies in the ability to find new and interesting systems whereby simple and rapid label-free monitoring, especially on supported lipid bilayers, can offer insight.

**A Few Comments on Microfluidics.** Throughout the course of this research, microfluidic devices have been utilized extensively. It is safe to assume that over a thousand individual devices have been produced and utilized, and some interesting observations warrant mentioning here. Firstly, it has been noticed that, in the case of pH-sensitive fluorophore-doped bilayers in microfluidic channels, the continuous flowing of buffer becomes important for maintaining the pH within the channel, especially as one drifts further from the buffering region of a particular buffering species. It was noticed that when fluid flow was stopped, the fluorescence intensity of pH-sensitive fluorophores in bilayers would begin to drift in a manner that suggested a gradual

lowering of solution pH. As can be seen in Figure 6.1, bilayers containing fluorescein dye, which fluoresces at high pH but is less fluorescent at lower pH, can be seen to drop in fluorescence intensity as flow through the microfluidic channel is stopped. When flow is resumed, the intensity quickly rises to the initial value, until flow is again stopped and the intensity begins to fall. This can also be observed in Figure 6.2, where the fluorescence intensity of bilayers containing *ortho*-Texas Red DHPE, which fluoresces it lower pH values but loses its fluorescence as it is deprotonated, is observed to increase with time in static microfluidic channels. These bilayers are being buffered by 10 mM PBS and as can be seen, the further one is from the buffering range of this species, the more intense the change in fluorescence observed upon stopping the flow. The behavior of these two fluorescent species suggests that with stopped flow, a volume such as is contained within a microfluidic channel (less than 1 μL in this case) is extremely susceptible to pH drift, most likely from $CO_2$ navigating through the semi-porous PDMS, though this is yet to be confirmed.

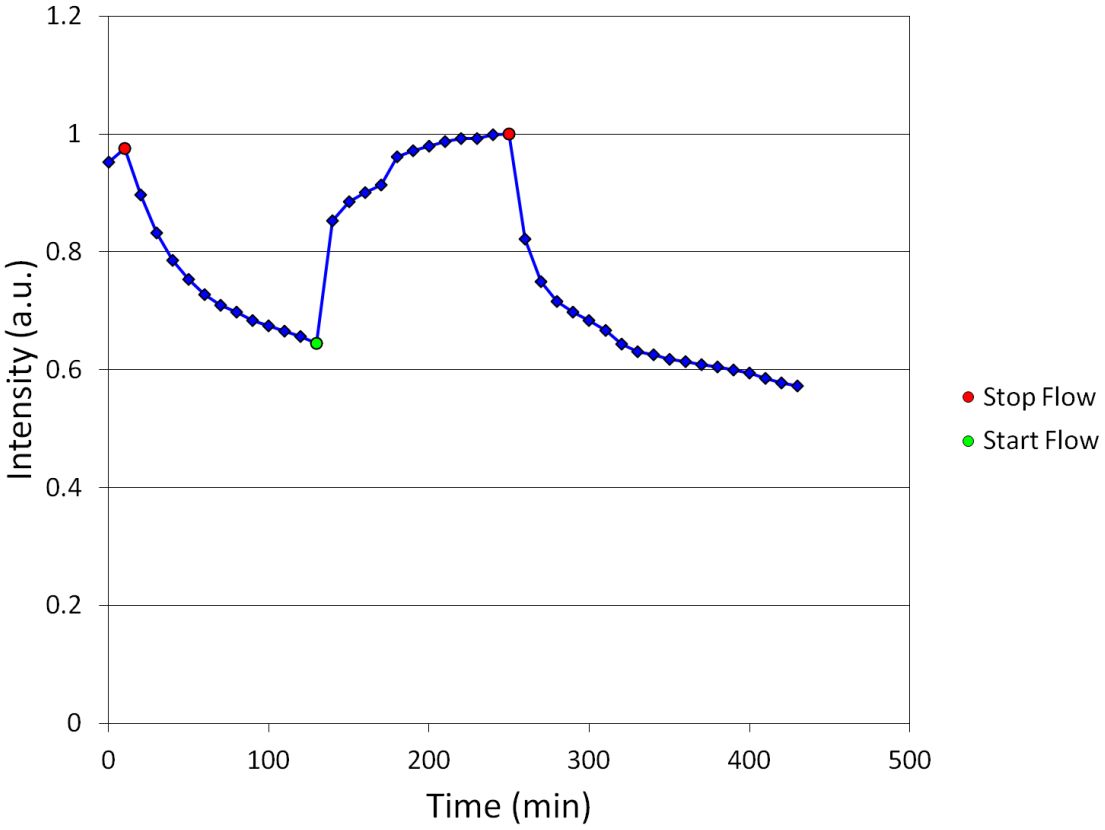


***Figure 6.1.*** Fluorescence Intensity Data with Start and Stop Flow**.** Fluorescence intensity measurements for fluorescein-labeled phospholipid in a supported lipid bilayer within a microfluidic channel. Green and red circles represent time at which the flow of buffer (10 mM PBS with 150 mM NaCl at pH 9.7) was started and stopped, respectively.

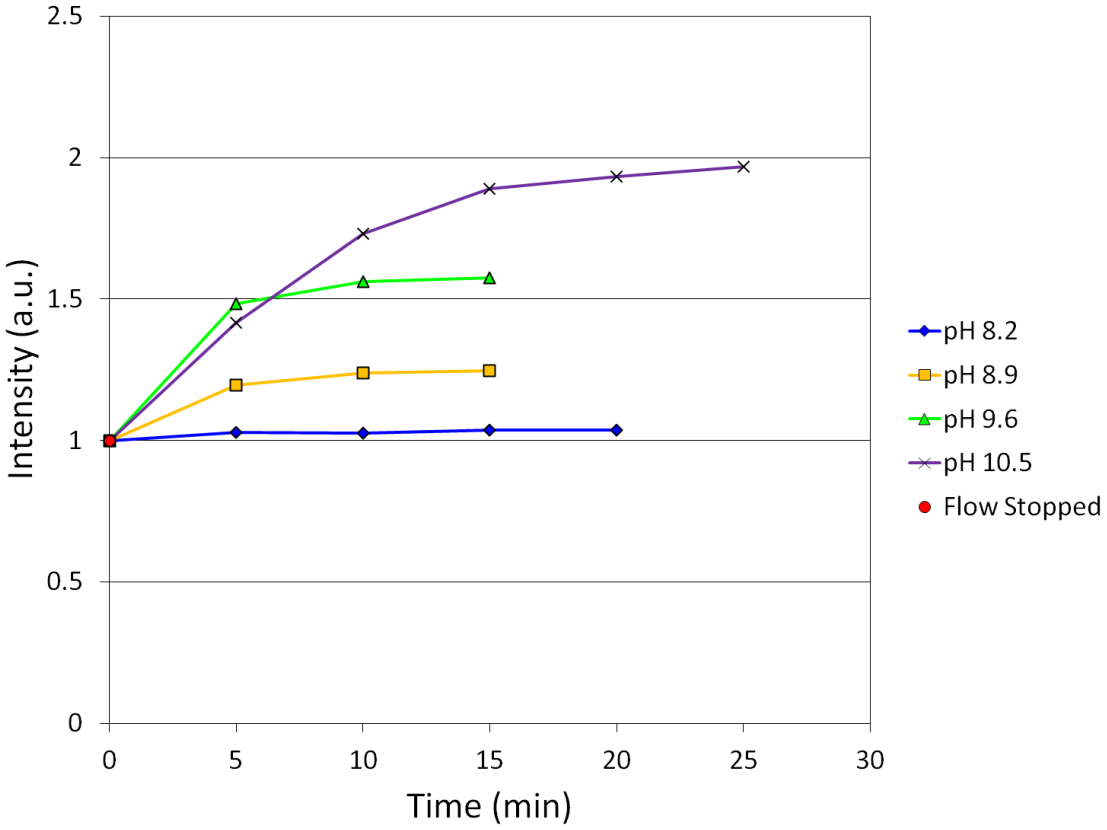


***Figure 6.2.*** Fluorescence Intensity Data with Stopped Flow at Different pH's. Fluorescence intensity measurements for *ortho*-rhodamine B POPE-containing bilayers in microfluidic channels after flow of 10 mM PBS buffer with 150 mM NaCl at various pH values had been stopped.

Additionally, it is interesting to note that the small dimensions of a microfluidic channel have an effect on the apparent pKa values of pH-responsive dyes, as can be seen from Figure 6.3. In a microfluidic device, a bilayer consisting of 0.5 mol% *ortho*-rhodamine B POPE, 30 mol% POPG and 69.5 mol% POPC the apparent pKa of the fluorophore in 10 mM PBS with 150 mM NaCl is about 7.3, whereas the same system in a flow cell has a slightly lower pKa value of 7.1. While this shift may not seem significant, it speaks to the highly confined nature of a microfluidic channel, where it is apparent that the deprotonation of the fluorophore requires a slightly more basic bulk solution. Such subtleties in the differences between bilayers in microfluidics and otherwise require a more thorough investigation than the few observations presented here, and may lead to some interesting and useful biophysical observations.

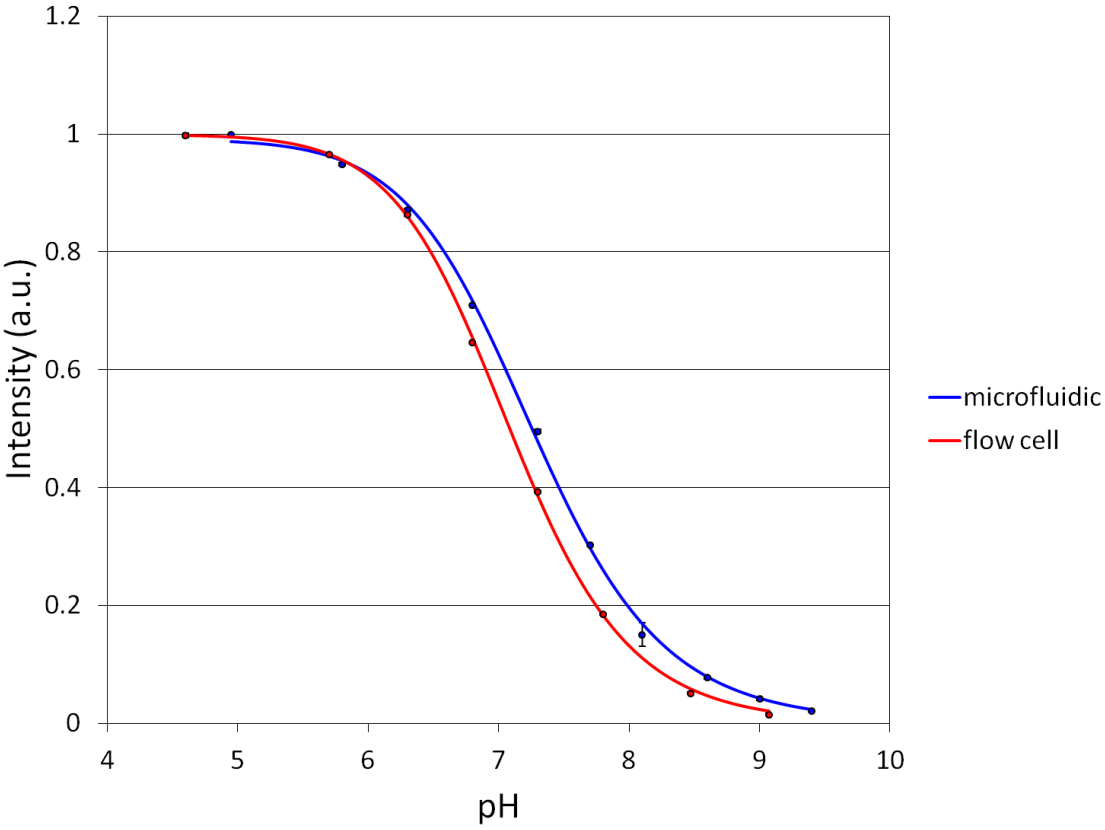


***Figure 6.3.*** Comparison of pH Titration in Microfluidic and Flow Cell. Comparison of pH titration curves for bilayers composed of 0.5 mol% *ortho*-rhodamine B POPE, 30 mol% POPG, and 69.5 mol% POPC in both a microfluidic device and a flow cell. 10 mM PBS with 150 mM NaCl was used in both titrations.

# REFERENCES


(1) Christopoulos, A. *Nat Rev Drug Discov* **2002**, *1*, 198.

(2) Mammen, M.; Choi, S. K.; Whitesides, G. M. *Angew Chem Int Edit* **1998**, *37*, 2755.

(3) Stace, C. L.; Ktistakis, N. T. *Bba-Mol Cell Biol L* **2006**, *1761*, 913.

(4) Kim, J. Y.; Mosior, M.; Chung, L. A.; Wu, H.; Mclaughlin, S. *Biophys J* **1991**, *60*, 135.

(5) Axelrod, D.; Burghardt, T. P.; Thompson, N. L. *Annual review of biophysics and bioengineering* **1984**, *13*, 247.

(6) Pisarchick, M. L.; Thompson, N. L. *Biophys J* **1990**, *58*, 1235.

(7) Soper, S. A.; Warner, I. M.; McGown, L. B. *Anal Chem* **1998**, *70*, 477r.

(8) Yang, T.; Baryshnikova, O. K.; Mao, H.; Holden, M. A.; Cremer, P. S. *J Am Chem Soc* **2003**, *125*, 4779.

(9) Jung, H. S.; Yang, T.; Lasagna, M. D.; Shi, J. J.; Reinhart, G. D.; Cremer, P. S. *Biophys J* **2008**, *94*, 3094.

(10) Kodadek, T. *Chem Biol* **2001**, *8*, 105.

(11) Yu, X. B.; Xu, D. K.; Cheng, Q. *Proteomics* **2006**, *6*, 5493.

(12) Murray, D.; Arbuzova, A.; Hangyas-Mihalyne, G.; Gambhir, A.; Ben-Tal, N.; Honig, B.; McLaughlin, S. *Biophys J* **1999**, *77*, 3176.

(13) Yang, C. Y.; Brooks, E.; Li, Y.; Denny, P.; Ho, C. M.; Qi, F. X.; Shi, W. Y.; Wolinsky, L.; Wu, B.; Wong, D. T. W.; Montemagno, C. D. *Lab Chip* **2005**, *5*, 1017.

(14) Anker, J. N.; Hall, W. P.; Lambert, M. P.; Velasco, P. T.; Mrksich, M.; Klein, W. L.; Van Duyne, R. P. *J Phys Chem C* **2009**, *113*, 5891.

(15) Das, A.; Zhao, J.; Schatz, G. C.; Sligar, S. G.; Van Duyne, R. P. *Anal Chem* **2009**, *81*, 3754.

(16) Wegner, G. J.; Lee, H. J.; Corn, R. M. *Anal Chem* **2002**, *74*, 5161.

(17) Yang, X.; Gu, C.; Qian, F.; Li, Y.; Zhang, J. Z. *Anal Chem* **2011**, *83*, 5888.

(18) Armani, A. M.; Kulkarni, R. P.; Fraser, S. E.; Flagan, R. C.; Vahala, K. J. *Science* **2007**, *317*, 783.

(19) Washburn, A. L.; Gunn, L. C.; Bailey, R. C. *Anal Chem* **2009**, *81*, 9499.

(20) Cooper, M. A.; Dultsev, F. N.; Minson, T.; Ostanin, V. P.; Abell, C.; Klenerman, D. *Nat Biotechnol* **2001**, *19*, 833.

(21) Furusawa, H.; Komatsu, M.; Okahata, Y. *Anal Chem* **2009**, *81*, 1841.

(22) Muratsugu, M.; Ohta, F.; Miya, Y.; Hosokawa, T.; Kurosawa, S.; Kamo, N.; Ikeda, H. *Anal Chem* **1993**, *65*, 2933.

(23) Cooper, M. A.; Singleton, V. T. *J Mol Recognit* **2007**, *20*, 154.

(24) Wang, W. U.; Chen, C.; Lin, K. H.; Fang, Y.; Lieber, C. M. *P Natl Acad Sci USA* **2005**, *102*, 3208.

(25) Patolsky, F.; Zheng, G. F.; Lieber, C. M. *Anal Chem* **2006**, *78*, 4260.

(26) Zheng, G. F.; Patolsky, F.; Lieber, C. M. *Abstr Pap Am Chem S* **2005**, *229*, U782.

(27) Kim, A.; Ah, C. S.; Yu, H. Y.; Yang, J. H.; Baek, I. B.; Ahn, C. G.; Park, C. W.; Jun, M. S.; Lee, S. *Appl Phys Lett* **2007**, *91*.

(28) Backmann, N.; Zahnd, C.; Huber, F.; Bietsch, A.; Pluckthun, A.; Lang, H. P.; Guntherodt, H. J.; Hegner, M.; Gerber, C. *P Natl Acad Sci USA* **2005**, *102*, 14587.

(29) Wee, K. W.; Kang, G. Y.; Park, J.; Kang, J. Y.; Yoon, D. S.; Park, J. H.; Kim, T. S. *Biosens Bioelectron* **2005**, *20*, 1932.

(30) Wu, G. H.; Datar, R. H.; Hansen, K. M.; Thundat, T.; Cote, R. J.; Majumdar, A. *Nat Biotechnol* **2001**, *19*, 856.

(31) Hwang, K. S.; Lee, J. H.; Park, J.; Yoon, D. S.; Park, J. H.; Kim, T. S. *Lab Chip* **2004**, *4*, 547.

(32) Song, X. D.; Swanson, B. I. *Anal Chem* **1999**, *71*, 2097.

(33) Jung, H.; Robison, A. D.; Cremer, P. S. *J Am Chem Soc* **2009**, *131*, 1006.

(34) Cremer, P. S.; Boxer, S. G. *J Phys Chem B* **1999**, *103*, 2554.

(35) von Heijne, G. *The Journal of membrane biology* **1990**, *115*, 195.

(36) Bishop, W. R.; Bell, R. M. *Annual review of cell biology* **1988**, *4*, 579.

(37) Opdenkamp, J. A. F. *Annu Rev Biochem* **1979**, *48*, 47.

(38) Schwarze, S. R.; Dowdy, S. F. *Trends Pharmacol Sci* **2000**, *21*, 45.

(39) Schwarze, S. R.; Hruska, K. A.; Dowdy, S. F. *Trends Cell Biol* **2000**, *10*, 290.

(40) Lindgren, M.; Hallbrink, M.; Prochiantz, A.; Langel, U. *Trends Pharmacol Sci* **2000**, *21*, 99.

(41) Wadia, J. S.; Dowdy, S. F. *Curr Opin Biotech* **2002**, *13*, 52.

(42) Yount, N. Y.; Yeaman, M. R. *P Natl Acad Sci USA* **2004**, *101*, 7363.

(43) Leventis, P. A.; Grinstein, S. *Annu Rev Biophys* **2010**, *39*, 407.

(44) Zwaal, R. F.; Comfurius, P.; Bevers, E. M. *Biochim Biophys Acta* **1998**, *1376*, 433.

(45) Swairjo, M. A.; Concha, N. O.; Kaetzel, M. A.; Dedman, J. R.; Seaton, B. A. *Nature structural biology* **1995**, *2*, 968.

(46) Sutton, R. B.; Sprang, S. R. *Structure* **1998**, *6*, 1395.

(47) Verdaguer, N.; Corbalan-Garcia, S.; Ochoa, W. F.; Fita, I.; Gomez-Fernandez, J. C. *Embo J* **1999**, *18*, 6329.

(48) Morales, K. A.; Lasagna, M.; Gribenko, A. V.; Yoon, Y.; Reinhart, G. D.; Lee, J. C.; Cho, W.; Li, P.; Igumenova, T. I. *J Am Chem Soc* **2011**, *133*, 10599.

(49) Monson, C. F.; Cong, X.; Robison, A. D.; Pace, H. P.; Liu, C. M.; Poyton, M. F.; Cremer, P. S. *J Am Chem Soc* **2012**, *134*, 7773.

(50) Brian, A. A.; Mcconnell, H. M. *P Natl Acad Sci-Biol* **1984**, *81*, 6159.

(51) Mcconnell, H. M.; Watts, T. H.; Weis, R. M.; Brian, A. A. *Biochim Biophys Acta* **1986**, *864*, 95.

(52) Kim, J.; Kim, G.; Cremer, P. S. *Langmuir* **2001**, *17*, 7255.

(53) Yang, T. L.; Jung, S. Y.; Mao, H. B.; Cremer, P. S. *Anal Chem* **2001**, *73*, 165.

(54) Duffy, D. C.; McDonald, J. C.; Schueller, O. J. A.; Whitesides, G. M. *Anal Chem* **1998**, *70*, 4974.

(55) Shi, J. J.; Yang, T. L.; Kataoka, S.; Zhang, Y. J.; Diaz, A. J.; Cremer, P. S. *J Am Chem Soc* **2007**, *129*, 5954.

(56) Delamarche, E.; Schmid, H.; Michel, B.; Biebuyck, H. *Adv Mater* **1997**, *9*, 741.

(57) Bocquet, L.; Barrat, J. L. *Soft Matter* **2007**, *3*, 685.

(58) Xia, Y. N.; Whitesides, G. M. *Angew Chem Int Edit* **1998**, *37*, 551.

(59) Paguirigan, A. L.; Beebe, D. J. *Integr Biol* **2009**, *1*, 182.

(60) Tamm, L. K.; Mcconnell, H. M. *Biophys J* **1985**, *47*, 105.

(61) Yi, F.; Xu, J.; Smith, A. M.; Parikh, A. N.; Lavan, D. A. *Soft Matter* **2009**, *5*, 5037.

(62) Shen, S. K.; Kendall, E.; Oliver, A.; Ngassam, V.; Hu, D. D.; Parikh, A. N. *Soft Matter* **2011**, *7*, 1001.

(63) Ma, C.; Srinivasan, M. P.; Waring, A. J.; Lehrer, R. I.; Longo, M. L.; Stroeve, P. *Colloid Surface B* **2003**, *28*, 319.

(64) Diaz, A. J.; Albertorio, F.; Daniel, S.; Cremer, P. S. *Langmuir* **2008**, *24*, 6820.

(65) Wagner, M. L.; Tamm, L. K. *Biophys J* **2000**, *79*, 1400.

(66) Giess, F.; Friedrich, M. G.; Heberle, J.; Naumann, R. L.; Knoll, W. *Biophys J* **2004**, *87*, 3213.

(67) V, A.; Knorr, N.; Duran, R. S.; Ingebrandt, S.; Offenhausser, A.; Knoll, W.; I, K. *Biophys J* **2005**, *89*, 1780.

(68) Taylor, J. D.; Linman, M. J.; Wilkop, T.; Cheng, Q. *Anal Chem* **2009**, *81*, 1146.

(69) Han, X. J.; Achalkumar, A. S.; Bushby, R. J.; Evans, S. D. *Chem-Eur J* **2009**, *15*, 6363.

(70) Junghans, A.; Champagne, C.; Cayot, P.; Loupiac, C.; Koper, I. *Langmuir* **2011**, *27*, 2709.

(71) Corrie, J. E. T.; Davis, C. T.; Eccleston, J. F. *Bioconjugate Chem* **2001**, *12*, 186.

(72) Corrie, J. E. T.; Eccleston, J. F.; Ferenczi, M. A.; Moore, M. H.; Turkenburg, J. P.; Trentham, D. R. *J Phys Org Chem* **2008**, *21*, 286.

(73) Skander, M.; Humbert, N.; Collot, J.; Gradinaru, J.; Klein, G.; Loosli, A.; Sauser, J.; Zocchi, A.; Gilardoni, F.; Ward, T. R. *J Am Chem Soc* **2004**, *126*, 14411.

(74) Green, N. M. *Method Enzymol* **1990**, *184*, 51.

(75) Monson, C. F.; Pace, H. P.; Liu, C. M.; Cremer, P. S. *Anal Chem* **2011**, *83*, 2090.

(76) Israelachvili, J. N. *Intermolecular and Surface Forces*; 3rd ed.; Elsevier, 2011.

(77) Metzler, D. E.; Metzler, C. M. *Biochemistry: the chemical reactions of living cells*; Harcourt/Academic Press, 2001.

(78) Hartmann, E.; Rapoport, T. A.; Lodish, H. F. *P Natl Acad Sci USA* **1989**, *86*, 5786.

(79) Nilsson, I. M.; Vonheijne, G. *Cell* **1990**, *62*, 1135.

(80) Ross, A. H.; Radhakrishnan, R.; Robson, R. J.; Khorana, H. G. *J Biol Chem* **1982**, *257*, 4152.

(81) Kim, J. Y.; Blackshear, P. J.; Johnson, J. D.; Mclaughlin, S. *Biophys J* **1994**, *67*, 227.

(82) Arbuzova, A.; Wang, L. B.; Wang, J. Y.; Hangyas-Mihalyne, G.; Murray, D.; Honig, B.; McLaughlin, S. *Biochemistry-Us* **2000**, *39*, 10330.

(83) Mosior, M.; Mclaughlin, S. *Biophys J* **1991**, *60*, 149.

(84) Cohen, A. M.; Liu, S. C.; Lawler, J.; Derick, L.; Palek, J. *Biochemistry-Us* **1988**, *27*, 614.

(85) Zhou, W. J.; Parent, L. J.; Wills, J. W.; Resh, M. D. *J Virol* **1994**, *68*, 2556.

(86) Blondelle, S. E.; Lohner, K.; Aguilar, M. I. *Bba-Biomembranes* **1999**, *1462*, 89.

(87) Epand, R. M.; Vogel, H. J. *Bba-Biomembranes* **1999**, *1462*, 11.

(88) Rapaport, D.; Shai, Y. *J Biol Chem* **1991**, *266*, 23769.

(89) Ludtke, S. J.; He, K.; Heller, W. T.; Harroun, T. A.; Yang, L.; Huang, H. W. *Biochemistry-Us* **1996**, *35*, 13723.

(90) Wimley, W. C. *Acs Chem Biol* **2010**, *5*, 905.

(91) Gazit, E.; Miller, I. R.; Biggin, P. C.; Sansom, M. S. P.; Shai, Y. *J Mol Biol* **1996**, *258*, 860.

(92) Bechinger, B.; Lohner, K. *Bba-Biomembranes* **2006**, *1758*, 1529.

(93) Arias, C. A.; Murray, B. E. *New Engl J Med* **2009**, *360*, 439.

(94) Koren, E.; Torchilin, V. P. *Trends Mol Med* **2012**, *18*, 385.

(95) Ryser, H. J. P.; Hancock, R. *Science* **1965**, *150*, 501.

(96) Green, M.; Loewenstein, P. M. *Cell* **1988**, *55*, 1179.

(97) Frankel, A. D.; Pabo, C. O. *Cell* **1988**, *55*, 1189.

(98) Vives, E.; Brodin, P.; Lebleu, B. *J Biol Chem* **1997**, *272*, 16010.

(99) Abes, R.; Arzumanov, A. A.; Moulton, H. M.; Abes, S.; Ivanova, G. D.; Iversen, P. L.; Gait, M. J.; Lebleu, B. *Biochem Soc Trans* **2007**, *35*, 775.

(100) Lindgren, M.; Langel, U. *Methods Mol Biol* **2011**, *683*, 3.

(101) Hudecz, F.; Banoczi, Z.; Csik, G. *Med Res Rev* **2005**, *25*, 679.

(102) Stewart, K. M.; Horton, K. L.; Kelley, S. O. *Org Biomol Chem* **2008**, *6*, 2242.

(103) Mosior, M.; Mclaughlin, S. *Biochim Biophys Acta* **1992**, *1105*, 185.

(104) Ben-Tal, N.; Honig, B.; Peitzsch, R. M.; Denisov, G.; McLaughlin, S. *Biophys J* **1996**, *71*, 561.

(105) Hoernke, M.; Schwieger, C.; Kerth, A.; Blume, A. *Bba-Biomembranes* **2012**, *1818*, 1663.

(106) Vazdar, M.; Vymetal, J.; Heyda, J.; Vondrasek, J.; Jungwirth, P. *J Phys Chem A* **2011**, *115*, 11193.

(107) Xia, Y. N.; McClelland, J. J.; Gupta, R.; Qin, D.; Zhao, X. M.; Sohn, L. L.; Celotta, R. J.; Whitesides, G. M. *Adv Mater* **1997**, *9*, 147.

(108) Roux, M.; Neumann, J. M.; Bloom, M.; Devaux, P. F. *Eur Biophys J Biophy* **1988**, *16*, 267.

(109) Bonev, B.; Watts, A.; Bokvist, M.; Grobner, G. *Phys Chem Chem Phys* **2001**, *3*, 2904.

(110) Mitchell, D. J.; Kim, D. T.; Steinman, L.; Fathman, C. G.; Rothbard, J. B. *J Pept Res* **2000**, *56*, 318.

(111) Futaki, S.; Suzuki, T.; Ohashi, W.; Yagami, T.; Tanaka, S.; Ueda, K.; Sugiura, Y. *J Biol Chem* **2001**, *276*, 5836.

(112) Wender, P. A.; Mitchell, D. J.; Pattabiraman, K.; Pelkey, E. T.; Steinman, L.; Rothbard, J. B. *P Natl Acad Sci USA* **2000**, *97*, 13003.

(113) Tang, M.; Waring, A. J.; Hong, M. *J Am Chem Soc* **2007**, *129*, 11438.

(114) Magalhaes, A.; Maigret, B.; Hoflack, J.; Gomes, J. A. N. F.; Scheraga, H. A. *J Protein Chem* **1994**, *13*, 195.

(115) Vondrasek, J.; Mason, P. E.; Heyda, J.; Collins, K. D.; Jungwirth, P. *J Phys Chem B* **2009**, *113*, 9041.

(116) Mason, P. E.; Neilson, G. W.; Enderby, J. E.; Saboungi, M. L.; Dempsey, C. E.; MacKerell, A. D.; Brady, J. W. *J Am Chem Soc* **2004**, *126*, 11462.

(117) Fadok, V. A.; Voelker, D. R.; Campbell, P. A.; Cohen, J. J.; Bratton, D. L.; Henson, P. M. *J Immunol* **1992**, *148*, 2207.

(118) Balasubramanian, K.; Mirnikjoo, B.; Schroit, A. J. *J Biol Chem* **2007**, *282*, 18357.

(119) Mirnikjoo, B.; Balasubramanian, K.; Schroit, A. J. *J Biol Chem* **2009**, *284*, 22512.

(120) Williamson, P.; Bevers, E. M.; Smeets, E. F.; Comfurius, P.; Schlegel, R. A.; Zwaal, R. F. *Biochemistry-Us* **1995**, *34*, 10448.

(121) Macedo-Ribeiro, S.; Bode, W.; Huber, R.; Quinn-Allen, M. A.; Kim, S. W.; Ortel, T. L.; Bourenkov, G. P.; Bartunik, H. D.; Stubbs, M. T.; Kane, W. H.; Fuentes-Prior, P. *Nature* **1999**, *402*, 434.

(122) Huang, M. D.; Rigby, A. C.; Morelli, X.; Grant, M. A.; Huang, G. Q.; Furie, B.; Seaton, B.; Furie, B. C. *Nature structural biology* **2003**, *10*, 751.

(123) Newton, A. C. *Chem Rev* **2001**, *101*, 2353.

(124) Steinberg, S. F. *Physiol Rev* **2008**, *88*, 1341.

(125) Manna, D.; Bhardwaj, N.; Vora, M. S.; Stahelin, R. V.; Lu, H.; Cho, W. H. *J Biol Chem* **2008**, *283*, 26047.

(126) Elam, J. S.; Thomas, S. T.; Holloway, S. P.; Taylor, A. B.; Hart, P. J. *Adv Protein Chem* **2002**, *60*, 151.

(127) Linder, M. C.; HazeghAzam, M. *Am J Clin Nutr* **1996**, *63*, S797.

(128) Rosse, C.; Linch, M.; Kermorgant, S.; Cameron, A. J. M.; Boeckeler, K.; Parker, P. J. *Nat Rev Mol Cell Bio* **2010**, *11*, 103.

(129) Rae, T. D.; Schmidt, P. J.; Pufahl, R. A.; Culotta, V. C.; O'Halloran, T. V. *Science* **1999**, *284*, 805.